

ANALYSIS OF CHLORIDE PROCESS REACTORS
FOR THE REDUCTION OF OXIDE SCALE
THROUGH COMPUTATIONAL FLUID
DYNAMICS

By

MARY ANN ROSS

Bachelor of Science

Oklahoma State University

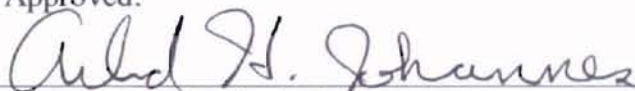
Stillwater, Oklahoma

1998

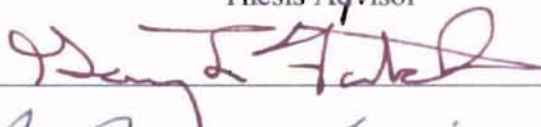
Submitted to the Faculty of the
Graduate College of
Oklahoma State University
in partial fulfillment of
the requirements for
the Degree of
MASTER OF SCIENCE
May 2001

ANALYSIS OF CHLORIDE PROCESS REACTORS
FOR THE REDUCTION OF OXIDE SCALE
THROUGH COMPUTATIONAL FLUID
DYNAMICS

Thesis Approved:



Thesis Advisor







Dean of the Graduate College

PREFACE

The goal of this research is to evaluate the efficacy of the hot-gas sheathe design concept in reducing oxide scale in chloride process reactors. Titanium dioxide wall deposition poses several concerns for the pigment industry. Oxide scale quickly forms in the reactor and, depending on design, possibly on the reactant inlet nozzles plugging the reactor and causing shutdown of the process for cleaning. The oxide scale growth also causes the flow of gases to be diverted thereby hindering effective mixing and complete reaction. Additionally, during scale growth, chunks of scale can break away causing difficulty in recovering fine uniform titanium dioxide particles.

I would like to express my gratitude to my graduate advisors, Dr. Arland Johannes and Dr. Gary Foutch, for the opportunity to take part in this research. I would also like to thank Dr. Afshin Ghajar for his dedicated involvement in this project and for serving on my committee. The dedication, support, and leadership of these three individuals are deeply appreciated.

I would also like to thank my fellow students and teammates on this project, Brant Aggus and Jae-Yong Kim. Their unlimited teamwork and cooperation helped make this research a very rewarding experience. Dennis Hussey and Chris Schult were also a great help to me with their computer and technical expertise.

I would especially like to thank Kerr-McGee Corporation, specifically Dr. Bill Yuill and Dr. Chuck Natalie. The opportunity to work on this project has been highly

rewarding and I hope to provide applicable insight on gas-blanketed reactors. Financial assistance provided by Kerr-McGee Corporation is also appreciated.

Most of all, I would like to thank my parents Ralph and Harriet Ross who are extremely supportive in all my endeavors and my fiancé, Steve, for his patience and encouragement.

TABLE OF CONTENTS

Chapter	Page
I INTRODUCTION	1
Titanium Dioxide	1
Chloride Process.....	2
Objectives	3
II LITERATURE REVIEW.....	4
Introduction.....	4
Titanium Dioxide	4
Manufacture of Titanium Dioxide.....	7
Patented Reactor Designs	9
United States Patent #2,670,272.....	9
United States Patent #3,284,159.....	10
United States Patent #3,203,762.....	11
United States Patent #3,311,452.....	12
United States Patent #3,351,427.....	14
United States Patent #3,586,055.....	15
United States Patent #3,676,060.....	15
United States Patent #3,725,526.....	16
Summary.....	17
III CFD ANALYSES	18
Introduction.....	18
Fluid Mechanics Equations.....	18
Mass Balance.....	19
Momentum Balance.....	19
Energy Balance.....	20
Analyses of Chloride Process Reactors	21
Cabot Reactor Patent # 3,311,452	25
PPG Industries Reactor Patent # 3,586,055	30
Kerr-McGee Corporation Reactor.....	32
Altered Kerr-McGee Reactor with Gas Blanket	34
Summary.....	35
IV RESULTS OF CFD ANALYSES.....	36
Introduction.....	36
Cabot Reactor Patent # 3,311,452.....	36
PPG Industries Reactor Patent # 3,586,055.....	46
Kerr-McGee Corporation Reactor.....	52

Chapter	Page
V CONCLUSIONS AND RECOMMENDATIONS.....	60
Cabot Reactor Patent # 3,311,452.....	60
PPG Industries Reactor Patent # 3,586,055.....	61
Kerr-McGee Reactor	61
REFERENCES.....	63
APPENDIX A.....	66
Additional Cabot Results	66
CASE I.....	66
CASE II.....	69
CASE III	72
CASE IV	75
APPENDIX B	79
Additional PPG Results	79
Low Chlorine Flow (Case I)	79
High Chlorine Flow (Case II).....	81
APPENDIX C	84
Additional Kerr-McGee Results.....	84
Original Kerr-McGee Reactor.....	84
Altered Kerr-McGee Reactor.....	86
APPENDIX D	89
Sensitivity of Diffusivity Constant.....	89

LIST OF FIGURES

Figure	Page
1 Reactor (Patent # 2,670,272).....	10
2 Reactor (Patent # 3,284,159).....	11
3 Reactor (Patent # 3,203,762).....	12
4 Reactor (Patent # 3,311,452).....	13
5 Reactor (Patent # 3,351,427).....	14
6 Reactor (Patent # 3,586,055).....	15
7 Reactor (Patent # 3,725,526).....	16
8 Cabot Reactor Specified by Patent.....	26
9 Cabot Reactor Analyzed.....	27
10 3-D Cabot Reactor.....	28
11 PPG Reactor (Solid View).....	30
12 PPG Reactor (Wireframe View).....	31
13 Solid KM Reactor (Front and Rear View).....	32
14 Wire Frame KM Reactor (Front and Rear View).....	33
15 Chloride and Chlorine Inlets of Gas-Blanketed KM Reactor.....	34
16 Cabot Reactor, Inlet Configuration.....	37
17 (Cabot Case I) Mole Fraction O_2	37
18 (Cabot Case I) Mole Fraction $TiCl_4$	38
19 (Cabot Case I) Mole Fraction Cl_2	38
20 (Cabot Case I) Mole Fraction TiO_2	39
21 (Cabot Case II) Mole Fraction O_2	40
22 (Cabot Case II) Mole Fraction $TiCl_4$	40
23 (Cabot Case II) Mole Fraction Cl_2	41
24 (Cabot Case II) Mole Fraction TiO_2	41
25 (Cabot Case III) Mole Fraction O_2	42
26 (Cabot Case III) Mole Fraction $TiCl_4$	42
27 (Cabot Case III) Mole Fraction Cl_2	43
28 (Cabot Case III) Mole Fraction TiO_2	43
29 (Cabot Case IV) Mole Fraction O_2	44
30 (Cabot Case IV) Mole Fraction $TiCl_4$	44
31 (Cabot Case IV) Mole Fraction Cl_2	45
32 (Cabot Case IV) Mole Fraction TiO_2	45
33 (PPG Reactor Case I) Mole Fraction O_2	47
34 (PPG Reactor Case I) Mole Fraction $TiCl_4$	48
35 (PPG Reactor Case I) Mole Fraction Cl_2	48
36 (PPG Reactor Case I) Mole Fraction TiO_2	49
37 (PPG Reactor Case II) Mole Fraction O_2	50

Figure	Page
38 (PPG Reactor Case II) Mole Fraction TiCl_4	50
39 (PPG Reactor Case II) Mole Fraction Cl_2	51
40 (PPG Reactor Case II) Mole Fraction TiO_2	51
41 KM Reactor Longitudinal 2-D Rendering	52
42 KM Reactor 2-D Rendering	52
43 Mole Fraction TiO_2 (KM Reactor-Longitudinal)	53
44 Mole Fraction TiO_2 (Altered KM Reactor-Longitudinal)	53
45 Mole Fraction TiO_2 (KM Reactor)	54
46 Mole Fraction TiO_2 (Altered KM Reactor)	54
47 Mole Fraction O_2 (KM Reactor)	55
48 Mole Fraction TiCl_4 (KM Reactor)	55
49 Mole Fraction O_2 (Altered KM Reactor)	56
50 Mole Fraction TiCl_4 (Altered KM Reactor)	56
51 TiO_2 Flow Rates vs. Distance Downstream Reactor	57
52 TiO_2 Mole Fraction in Downstream Reactor (Kerr-McGee)	58
53 TiO_2 Mole Fraction in Downstream Reactor (Altered Kerr-McGee)	58
54 (Cabot Case I) Density Profile	66
55 (Cabot Case I) Reaction Profile	67
56 (Cabot Case I) Close-up Mole Fraction TiO_2	67
57 (Cabot Case I) Pressure Profile	68
58 (Cabot Case I) Velocity Profile	68
59 (Cabot Case I) Close-up Velocity Vector Profile	69
60 (Cabot Case II) Density Profile	69
61 (Cabot Case II) Pressure Profile	70
62 (Cabot Case II) Reaction Profile	70
63 (Cabot Case II) Velocity Profile	71
64 (Cabot Case II) Velocity Vector Profile	71
65 (Cabot Case II) Close-up Velocity Vector Profile	72
66 (Cabot Case III) Density Profile	72
67 (Cabot Case III) Pressure Profile	73
68 (Cabot Case III) Reaction Profile	73
69 (Cabot Case III) Velocity Profile	74
70 (Cabot Case III) Velocity Vector Profile	74
71 (Cabot Case III) Close-up Velocity Vector Profile	75
72 (Cabot Case IV) Density Profile	75
73 (Cabot Case IV) Pressure Profile	76
74 (Cabot Case IV) Reaction Profile	76
75 (Cabot Case IV) Velocity Profile	77
76 (Cabot Case IV) Velocity Vector Profile	77
77 (Cabot Case IV) Close-up Velocity Vector Profile	78
78 (PPG Reactor Case I) Density Profile	79
79 (PPG Reactor Case I) Pressure Profile	80
80 (PPG Reactor Case I) Reaction Profile	80
81 (PPG Reactor Case I) Velocity Profile	81

Figure	Page
82 (PPG Reactor Case I) Velocity Vector Profile.....	81
83 (PPG Reactor Case II) Density Profile	82
84 (PPG Reactor Case II) Pressure Profile	82
85 (PPG Reactor Case II) Reaction Profile	83
86 (PPG Reactor Case II) Velocity Profile.....	83
87 (Kerr-McGee Reactor) Density Profile	84
88 (Kerr-McGee Reactor) Pressure Profile	85
89 (Kerr-McGee Reactor) Reaction Profile.....	85
90 (Kerr-McGee Reactor) Velocity Profile	86
91 (Altered Kerr-McGee Reactor) Density Profile	86
92 (Altered Kerr-McGee Reactor) Pressure Profile	87
93 (Altered Kerr-McGee Reactor) Reaction Profile	87
94 (Altered Kerr-McGee Reactor) Velocity Profile.....	88
95 Mole Fraction of Titania (+50% Diffusivity)	89
96 Mole Fraction of Titania (-50% Diffusivity)	90

LIST OF TABLES

Table	Page
1 Fluid Properties (Fluent Inc.)	22
2 Density as a Function of Temperature.....	22
3 Cabot Analyses.....	27
4 Inlet Boundary Conditions CASE I.....	29
5 Inlet Boundary Conditions CASE II.....	29
6 Inlet Boundary Conditions CASE III	29
7 Inlet Boundary Conditions CASE IV	29
8 Inlet Boundary Conditions (PPG)	31
9 Inlet Boundary Conditions (Kerr-McGee).....	33
10 Cabot Reactor TiO ₂ Flow Rates	46

NOMENCLATURE

A	Titania particle surface area concentration (cm^2/cm^3)
C	Molar concentration of TiCl_4 (kmol/m^3)
$c_{p,j}'$	Heat capacity of species j' ($\text{kJ}/\text{mol K}$)
E	Activation energy (kJ/mol)
F_i	Momentum source term ($\text{kg}/\text{m}^2 \text{ s}^2$)
g_i	Gravitational forces in the i direction (m/s^2)
h	Enthalpy (kJ/kmol)
i	The i direction
i'	Species i'
j	The j direction
j'	Species j'
$J_{j'}$	Diffusion flux of species j' ($\text{kmol}/\text{m}^2 \text{ s}$)
k	Arrhenius rate constant (s^{-1})
k'	Rate constant ($\text{s}^{-1} \text{ mol}^{-1/2}$)
k_{eff}	Effective conductivity ($\text{kg m}/\text{s}^2 \text{ K}$)
k_s	Surface reaction rate constant (cm/s)
k_t	Turbulent thermal conductivity ($\text{kg m}/\text{s}^2 \text{ K}$)
M	Mass of system (kg)
p	Local static pressure (Pa)
R	Total rate of reaction (kmol/s)

R_g	Rate of reaction in gas phase (kmol/s)
R_s	Rate of reaction on solid surface (kmol/s)
S_h	Energy source term (kg/m ³ s ³)
S_m	Mass source term (kg/m ³ s)
t	Time (s)
T	Temperature (K)
u_i	Velocity in the i direction (m/s)
V	Volume of the mixture (m ³)
V_i'	Volume occupied by species i' (m ³)
x_i	Distance in the i direction (m)
ΔH	Heat of reaction (kJ/mol)
μ	Dynamic viscosity (kg/m s)
ρ	Density (kg/m ³)
τ_{ij}	Stress tensor (kg/m s ²)

CHAPTER I

INTRODUCTION

Titanium Dioxide

There is currently a large market for high quality ceramic powders such as titanium dioxide. Titanium dioxide, also called titania, is an essential aerosol component for the production of nearly seven billion pounds of white pigment per year (Braun, 1997). Titanium dioxide pigments are used in a variety of applications including paints, coatings, dyes, paper, plastics, and pharmaceuticals.

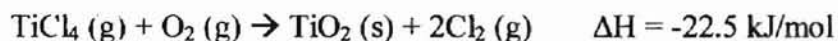
Titania pigments dominate the industry due to their enhanced opacity and lightness. Superior pigment performance of TiO_2 is rooted in the characteristics of the powder including particle size and shape, crystal phase, and composition. Titania particles have an extremely high refractive index (2.74 for rutile crystal phase and 2.55 for anatase) (Jain et al., 1997) therefore offering maximum light scattering with very little light absorption, a characteristic maximized between 0.15 and 0.25 micrometers particle size (Akhtar et al., 1991).

Pigment quality titanium dioxide must be manufactured from titanium ores: ilmenite (FeTiO_3), rutile (TiO_2), anatase (TiO_2), brookite (TiO_2), and leucoxene ($\text{TiO}_2 \cdot x\text{FeO} \cdot y\text{H}_2\text{O}$) (Braun, 1997). Once processed, the end product is in either the rutile crystal phase or the anatase phase. TiO_2 powders were initially produced in the anatase form, however, due to superior pigment performance of rutile and due to technological developments, it has nearly replaced the demand for anatase titania (Braun, 1997).

Chloride Process

There have been two major processes for the production of titanium dioxide; the sulfate process and the chloride process. The chloride process has largely taken the place of the sulfate process because it yields more rutile product and is more of a continuous, less labor-intensive method. Titanium dioxide particles produced in aerosol reactors via the chloride process have a narrower size distribution, a more spherical shape, and a higher purity. The chloride process also presents advantages in easier waste disposal and less energy consumption (Braun, 1997).

In the chloride process, titanium tetrachloride gas is reacted with hot oxygen to yield titanium dioxide powder and chlorine gas. The balanced chemical equation is as follows:



In many commercial aerosol reactors, excess preheated oxygen or oxygen-containing gas (between 800-1000 °C) is fed to the reactor in the presence of a plasma or liquid hydrocarbon-fed flame producing temperatures of 2500-3000 °C (Hartmann, 1993). Titanium tetrachloride (around 450 °C) is introduced downstream, and reacts with the hot oxygen to form titania particles. Hydrocarbon combustion products as well as titanium tetrachloride additives such as AlCl_3 serve to promote rutilization of the titanium dioxide (Powell, 1968).

The foremost problem with the chloride process is that many reactor designs have issues with oxide scale and growth quickly forming in the vicinity of the initial reaction and plugging inlet nozzles eventually causing shutdown of the process (Wilson, 1971). There are many patented reactor designs claiming to reduce or altogether eliminate oxide

scale on the reactor surface. Several patented solutions include porous walls, inert gas blankets at the reactor walls, cooled TiO_2 film on the reactor wall, and many different titanium tetrachloride nozzle designs.

Objectives

Kerr-McGee Corporation currently produces 535,000 tons per year of titanium dioxide, ranking Kerr-McGee as the third-largest producer of TiO_2 in the world (Kerr-McGee, 2000). To remain competitive on the titania market, Kerr-McGee has maintained continuous operation of their chloride process reactors by injecting sand into the reactor to prevent scale buildup. However, eventual shutdown of the process is necessary because the injected sand, scouring the internal reactor walls, wears down the reactor wall surface.

The objectives of this research are to identify possible causes of Kerr-McGee reactor oxide scale and to evaluate the potential of gas-blanketed reactor walls to reduce or eliminate scale using computational fluid dynamics (CFD). CFD is sophisticated computer software that thoroughly characterizes a real system by simultaneously performing mass, energy, momentum, and species balances on the system. Once solved, the solution presents a realistic two- or three-dimensional profile of the system including fluid velocities, pressures, temperatures, species concentrations and other profiles. The software package used for this research contains FLUENT 5 and the included CAD package, GAMBIT.

CHAPTER II

LITERATURE REVIEW

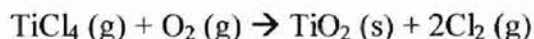
Introduction

In this chapter, several areas of research relating to titanium dioxide production through the chloride process are discussed. First, an overview of literature published on research involving the titanium dioxide reaction and particle growth mechanisms is presented. Next, a section is dedicated to a review of relevant publications on the manufacture of titanium dioxide. The final section is a review of several patented reactor designs with claims to reduce or eliminate particle accretion at the reactor walls.

Titanium Dioxide

Oxidation of titanium tetrachloride in an aerosol reactor at high temperatures and nearly atmospheric pressures, known as the chloride process, produces titanium dioxide powders, and is not completely understood since chemical reaction and particle growth occur rapidly (Pratsinis and Spicer, 1997). Several studies have been performed on the chloride process to produce more accurate models of the production and growth of titania particles. Specifically, the relative contributions of gas phase and surface reaction mechanisms, which yield titanium dioxide particles, have been researched at length.

The balanced oxidation reaction for titanium tetrachloride is:



TiCl₄ oxidation is carried out both on the solid surface and in the gas phase. The rate of reaction in the gas phase, R_g, and the rate of reaction on the solid surface, R_s, can be summed to achieve the overall reaction rate, R (Pratsinis and Spicer, 1998).

$$dC/dt = -R = -(R_g + R_s)$$

C is the concentration of TiCl₄ vapor. Pratsinis et al. (1990) measured the oxidation rate of TiCl₄ in a furnace aerosol reactor between temperatures of 700 and 1000 °C and initial TiCl₄/O₂ ratios between 1:1 and 1:20 in excess argon. They found that the overall reaction rate is first order with respect to TiCl₄ and zero order with respect to oxygen at lower oxygen concentrations. However, at ratios of 10:1 O₂/TiCl₄ and higher, the overall reaction rate was found to be half order with respect to oxygen.

$$-d[\text{TiCl}_4]/dt = (k + k' [\text{O}_2]^{1/2})[\text{TiCl}_4]$$

The Arrhenius rate constants are given as $k = 8.26 \times 10^4 \exp(-E/RT) \text{ s}^{-1}$ and $k' = 1.4 \times 10^5 \exp(-E/RT) (\text{L/mol})^{1/2} \text{ s}^{-1}$, where E is given as 88.8 +/- 3.2 kJ/mol (Pratsinis et al., 1990).

Pratsinis and Spicer (1998) define the rate of surface reaction, R_s, as follows:

$$R_s = k_s A [\text{TiCl}_4]$$

where $k_s = 4.9 \times 10^3 \exp(-8993/T) \text{ cm/s}$. A is the total titania particle surface area concentration (cm²/cm³) and is a complex function of particle diameter, velocity, and diffusivity.

There have been several publications with differing conclusions about the mechanism of particle growth of titania. Akhtar et al. (1991) studied experimentally the effects of temperature, reactant concentration, and residence time on particle size.

Particle size distributions were measured at reactor temperatures ranging from 1,200 K to 1,723 K, at initial chloride concentrations ranging from $9.34 \times 10^{-6} \text{ M}$ to $1.56 \times 10^{-5} \text{ M}$,

and residence times from 0.8 s to 1.6 s. When a coagulation enhancement factor is employed, the experimental results match closely with their theoretical predictions assuming gas phase reaction and coagulation. Furthermore, coagulation is the more significant growth mechanism due to the self-preserving size distribution in their hot-wall reactor (Akhtar et al., 1991). Jang and Jeong (1995) also studied the effects of reactor conditions on particle size. Experimental conditions ranged from 720 °C to 1000 °C reactor temperature and from 0.05 to 1.00 mol% titanium tetrachloride. They concluded that when reactants were not preheated to the reactor temperature, surface reaction kinetics has a propensity to increase the particle size distribution (Jang and Jeong, 1995). According to Jain et al. (1997), who took particle size measurements within the inlet chloride concentration range of 4.7×10^{-8} to 5.5×10^{-6} mol/cm³, reaction is not a significant growth mechanism relative to gas phase reaction and coagulation. These publications seem to hold differing conclusions about the mechanism of particle growth of titania

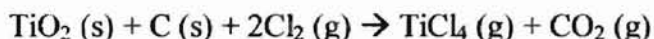
Finally, Pratsinis and Spicer (1998) claim to reconcile the differing opinions on particle growth by taking into account the inlet ratio of oxygen and titanium chloride. High titanium tetrachloride concentrations (nearly stoichiometric ratio of reactants) result in elevated concentrations of titania nuclei. High concentrations of TiO₂ nuclei allow greater surface area available for surface reactions to take place. If the reaction begins with or proceeds to having a low TiCl₄/O₂ ratio, then the gas phase reaction and coagulation dominate (Pratsinis and Spicer, 1998).

Manufacture of Titanium Dioxide

Manufacture of titanium dioxide through the chloride process involves the following steps:

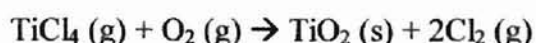
1. Titanium ore is chlorinated, producing a mixture of gases and unreacted solids.
2. Titanium tetrachloride is separated from solids and purified.
3. Titanium tetrachloride is oxidized in a high temperature flame reactor.
4. The pigment particles are finished with grinding and a thin aqueous coating (Braun, 1997).

Pulverized dry titanium ore and coke are reacted with hot chlorine between 900 °C and 1700 °C and slightly above atmospheric pressure. The chemical reaction occurs as follows:



Since this reaction is exothermic, the reactor requires cooling. The product gases are then removed from solids such as coke, titanium ore, iron chloride, and gangue (Braun, 1997). The titanium chloride gas stream is then condensed. Next, the liquid chloride solution is chemically treated to convert impurities to compounds that are either insoluble or have a higher boiling point than titanium tetrachloride that can then be purified by distillation (Powell, 1968). The TiCl_4 liquid is purified so that only a few parts per million of impurities remain in solution (Braun, 1997). Once the titanium tetrachloride is purified, it is then vaporized again and rutile-promoting additives such as AlCl_3 are added to the chloride. Very small concentrations of other metal ions may also be added to control titania particle size.

Titanium tetrachloride gas is then reacted continuously with excess hot oxygen to yield titanium dioxide powder and chlorine gas. The chemical reaction occurs as follows:



For a very rapid rate of reaction, heat is continually fed to the reactor in the form of a plasma or liquid hydrocarbon-fed flame producing temperatures of 2500-3000 °C (Hartmann, 1993). Titanium tetrachloride (around 450 °C) is commonly introduced downstream of the oxygen and reacts with the hot oxygen to form titania particles and chlorine gas. The reactor for this system must be designed to produce the desired particle size while avoiding particle deposition and buildup (Braun, 1997).

Most of the product chlorine is recycled to be used for the chlorination of the titanium ore. TiO_2 particles are mixed with water where residual chlorine and acids are removed. The titanium dioxide particles are then coated with a thin layer, only a few atoms thick, of a precipitation of oxyhydrates and oxides. Most common are the coatings of oxyhydrates of aluminum and silicon (Braun, 1997).

Lastly, the pigment particles are finished by dry grinding. Dry grinding does not break crystals into smaller submicron sized crystals because the bond strengths and density within the crystals are too high (Braun, 1997). Instead, the crystals are grown to the desired size in the aerosol reactor. The dry grinding process is intended to break apart agglomerations of crystals (Braun, 1997). The grinding is done by injecting the TiO_2 and possibly steam into a centrifugal device that causes the TiO_2 particles to collide and to break apart. Due to their higher mass, larger particles are forced to the outside edge where they continue to collide; smaller particles are ejected. The pigment is then separated and cooled (Braun, 1997).

Patented Reactor Designs

There are several patents available that present unique reactor designs and operating procedures for the production of titanium dioxide through the chloride process. These patents claim to reduce or eliminate oxide scale thereby achieving extended operation times. Several patented solutions include porous walls, inert gas blankets at the reactor walls, cooled TiO_2 film on the reactor wall, and many different titanium tetrachloride nozzle designs. This section is a review of several patented reactor designs with claims to reduce or eliminate particle accretion at the reactor walls.

United States Patent #2,670,272

E. I. du Pont de Nemours and Company (Nutting, 1954) patented a claim which presents a “effective method for continuously producing pigmentary titanium dioxide by the vapor phase oxidation at elevated temperatures of titanium tetrachloride without encountering objectional scale formation of deposition on the reactor surfaces and consequent apparatus plugging or inefficient operation” (U.S. patent # 2,670,272).

The design for this process is illustrated in Figure 1. Oxygen, or an oxygen containing gas, enters the reactor continuously through conduit 4 while titanium tetrachloride enters through conduit 11. Both gases are heated by furnace 2 and are mixed and reacted in conduit 6. A cool inert liquefied gas, normally chlorine or nitrogen, enters continuously through conduit 16 and into the reaction zone 6 through a porous refractory wall 7. The porous wall is intended for the purpose of reducing or eliminating oxide scale by:

1. Reducing mass transfer to the wall by means of an inert liquid being fed through the porous wall thereby shielding the reactor wall from the reacting gases.
 2. Keeping the reaction zone wall cool to prevent surface reaction at the wall.
- The rate of surface reaction is exponentially proportional to temperature.

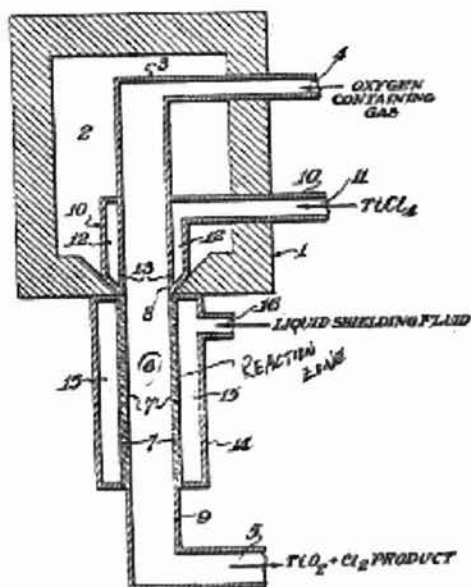


Figure 1 Reactor (Patent # 2,670,272)

United States Patent #3,284,159

E. I. du Pont de Nemours and Company (Kruse, 1966) proposed a similar reactor design for the production of TiO_2 . The difference between this design and the previous design is that the porous wall was eliminated and replaced with a reactor zone wall thinly coated with a metal oxide, preferably TiO_2 . The reactor zone wall is still cooled to prevent surface reaction at the wall. The thin layer of TiO_2 is added by spraying or

brushing an aqueous slurry of TiO_2 onto the wall surface. The purpose of the TiO_2 layer is to reduce contaminants in the pigment that come from corrosion of the reactor wall surfaces by the hot titanium chloride.

The reactor geometry is shown in Figure 2. Reactants enter the reactor, become heated, and exit the reactor as in patent US 2,670,272. The reaction zone is now surrounded with a cooling jacket 15 so that the reactor wall 7 is maintained between 450 °C and 500 °C, but not below 136 °C, the sublimation temperature of titanium tetrachloride (Powell, 1968).

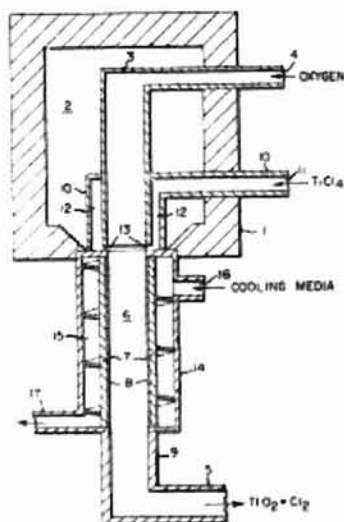


Figure 2 Reactor (Patent # 3,284,159)

United States Patent #3,203,762

Cabot Corporation (Carpenter, 1965) patented a reactor design that incorporated a flexible wall around the reaction zone that could liberate agglomerate continuously from the wall. Figure 3 illustrates the reactor design proposed in this patent. Referring to the design on the left of Figure 3, gas or liquid is introduced into pressure chamber 5 through conduit 7. As the pressure increases or decreases in chamber 5, wall 3 is caused to flex.

Wall 9 is solid. The more detailed design is included on the right in Figure 3. Oxygen and carbon monoxide are fed into the reactor through conduit 24 and combust to preheat reaction chamber 22. Additional oxygen and titanium tetrachloride are fed to the reaction chamber through conduit 28. Meanwhile, wall 10 is periodically caused to vibrate thereby loosening TiO_2 buildup accruing on the wall (Powell, 1968).

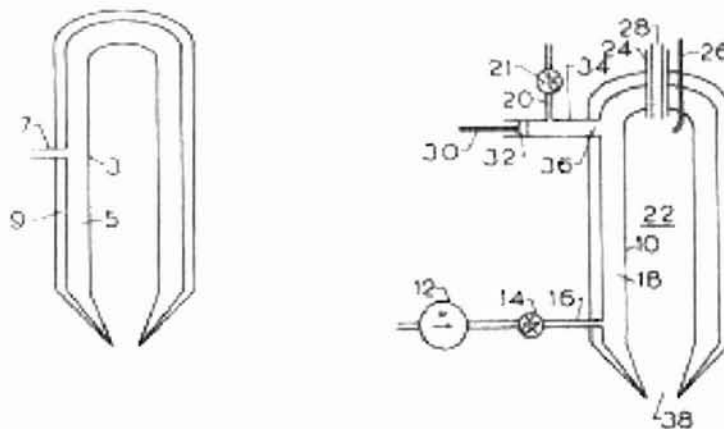


Figure 3 Reactor (Patent # 3,203,762)

United States Patent #3,311,452

Cabot Corporation (Goodgame, 1967) introduced a novel reactor design for the continuous production of titanium dioxide with minimal scale buildup. The reaction referenced in this process was the hydrolysis reaction of titanium tetrachloride; however, the reactor design is also useful for eliminating scale accrued through the oxidation of titanium tetrachloride. The concept employed in this patent is the use of an inert gas blanket to coat the reaction chamber wall. The gas blanket also serves as an additional source of heat for the hydrolysis or oxidation reaction.

Figure 4 is a two-dimensional illustration of this invention.

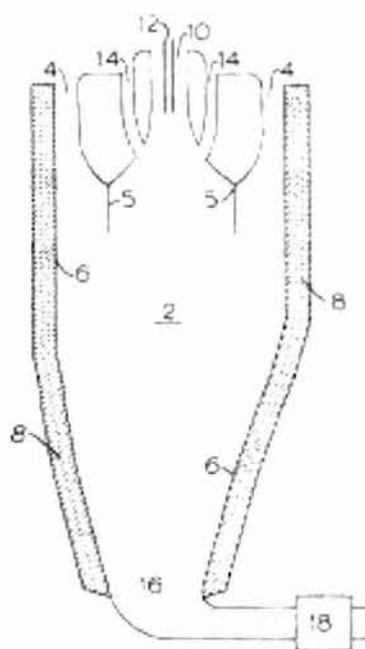
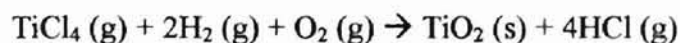


Figure 4 Reactor (Patent # 3,311,452)

Carbon monoxide and air are combusted and introduced into reaction chamber 2 through conduit 4 at a temperature of about 1200 °C. Titanium tetrachloride and dry air are introduced into the reaction chamber through conduit 10 while hydrogen is fed to the reactor through conduit 12. The hydrolysis reaction occurs in the reaction chamber 2 as follows:



The hot gas mixture entering through conduit 4 forms the protective gas blanket at the wall and must be supplied at a velocity equal to or greater than the velocity of the reacting fluid to prevent oxide scale (Goodgame et al., 1967). This patent is discussed in more detail in the following chapter.

United States Patent #3,351,427

Cabot Corporation (Wendell et al., 1967) proposed that a high velocity spinning mixture of reactants in a frusto-conical reactor design would eliminate oxide scaling. An illustration of the invention is shown in Figure 5.

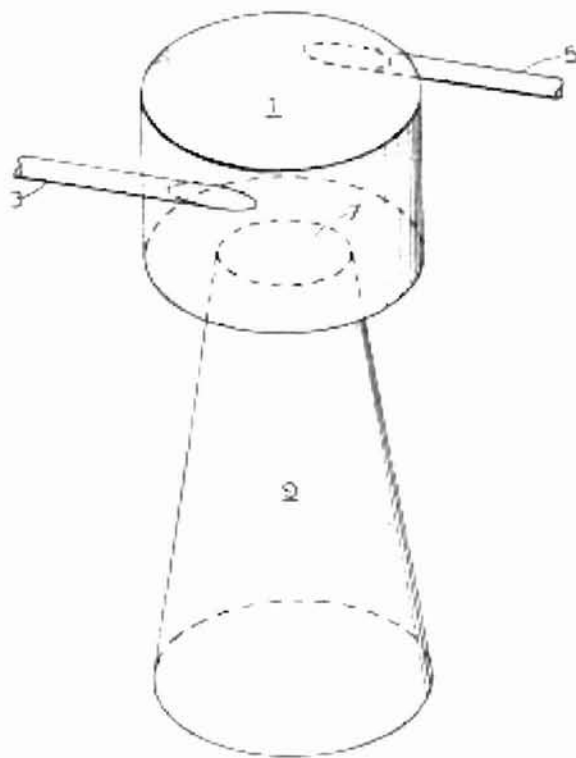


Figure 5 Reactor (Patent # 3,351,427)

Fuel gas and titanium tetrachloride are introduced into the reactor through conduit 5 while oxygen or an oxygen-containing gas is fed through conduit 3. Both inlet streams are fed at a linear velocity between 75 and 350 ft/s. When the reactant gases are fed into the reaction chamber 1 tangentially as shown in Figure 5, a spinning effect is induced therefore causing rapid mixing of the reactants. According to the inventors, this reactor design provides for higher reactant mixing which eliminates pockets of higher temperature and longer residence times (Powell, 1968).

United States Patent #3,586,055

PPG Industries (Wilson, 1971) proposed a method of introducing reactant gases into a reaction zone through concentric annuli separated by a stream of inert, usually chlorine gas, to force the reaction downstream of the physical inlets. Inlet distributor plates designed for the even distribution of gas in the inlet concentric tubes, combined with the hot gas stream, significantly reduce oxide scale on the reactor inlets. Figure 6 illustrates the configuration of the oxygen and inert gas inlets.

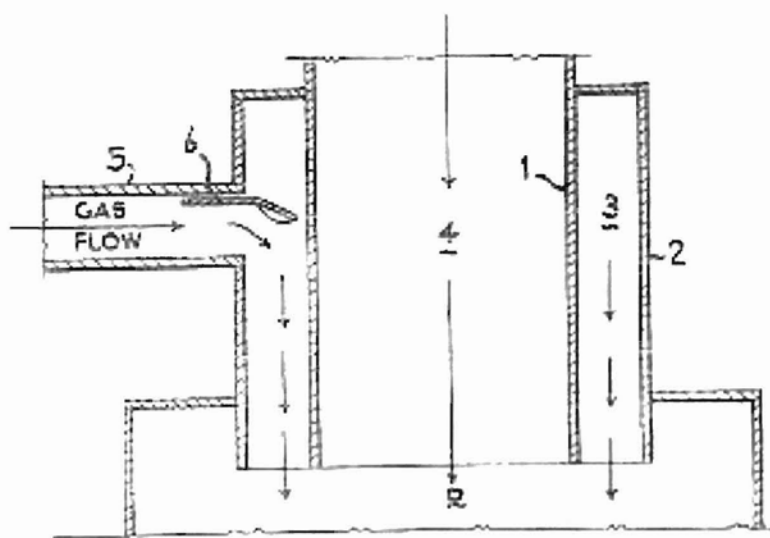


Figure 6 Reactor (Patent # 3,586,055)

Preheated oxygen flows downward through conduit 4 as chlorine and titanium tetrachloride is fed through two separate concentric annuli. The distributor plate 6 is added to insure more even flow through the annulus and more even mixing in the reaction zone. This patent is discussed in more detail in the following chapter.

United States Patent #3,676,060

Montecatini Edison (Bedetti, 1972) patented a reactor design that consisted of concentric annular inlets. The inner inlet is a mixture of hot oxygen and fuel while the

outer inlets are a relatively cool mixture of reactants. A recirculation zone is generated in the center of the reaction zone formed by the swirling flow of the inlet gases. This recirculation zone is maintained at an elevated temperature and heat is continuously fed to the passing reactants by conduction and convection. This patent also suggests a thin gas film coating the wall of the reactor meant for preventing oxide scale buildup.

United States Patent #3,725,526

Montecatini Edison (Pieri et al., 1973) patented another reactor design with a recirculation zone is maintained at an elevated temperature. Figure 7 is a two-dimensional illustration of their invention.

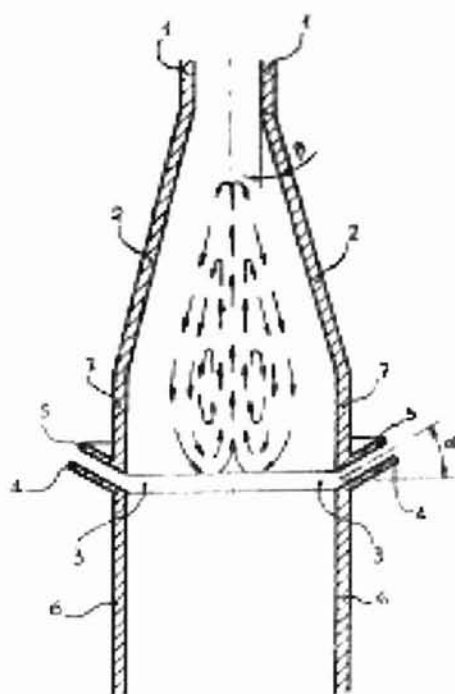


Figure 7 Reactor (Patent # 3,725,526)

Referring to Figure 7, hot preheated oxygen and fuel gas, usually carbon monoxide, at about 700 °C – 900 °C is fed through the annular conduit 1 into the combustion zone 2. The preheated oxidizing gas is passed through a helical vane to

induce a swirling effect. The oxygen/carbon monoxide mixture is burned in an auxiliary flame reaching a temperature of about 1,800 °C – 2,300 °C. Preheated titanium tetrachloride and a rutilizing agent are fed into the reactor through conduit 4 at an angle between 1 and 45 degrees. This patent says little about addressing the problem of product deposition in the reactor except that if the titanium tetrachloride stream were introduced upstream of the conical zone, the inclined wall is useful to prevent deposition.

Summary

This chapter discussed several areas of research relating to titanium dioxide production through the chloride process. Included in this chapter were a review of literature published involving research on the titanium dioxide reaction and particle growth mechanisms; a review of relevant publications on the manufacture of titanium dioxide; and a review of several patented reactor designs with claims to reduce or eliminate particle deposition on the reactor walls. Clearly, a hot gas layering the walls of the reaction chamber, either through annular or porous wall inlets, is a promising method of eliminating TiO₂ particle deposition in the reactor.

CHAPTER III

CFD ANALYSES

Introduction

Computational fluid dynamics (CFD) is sophisticated computer software that enables the study of fluid systems. CFD software simultaneously calculates mass, momentum, energy, and species transfer, as needed, to present a complete profile of the system of interest. To carry out these calculations, the program must first be furnished with the system geometry and boundary conditions. The geometry must then be meshed into an adequate, dense network of nodes where the calculations will be performed using a numerical integration technique.

The commercial CFD software used for this research is FLUENT 5. This software is designed to provide a rough estimate of the flow profiles of a system and is not intended to be used in determining the final design of equipment without additional analyses and experimentation (Fluent Incorporated, 1998).

This chapter begins with an overview of the transport equations used to model the aerosol reactor systems. Next, a description of the common analysis variables of the various gas-blanketed reactor systems is presented. Finally, the geometries and boundary conditions are presented for each reactor.

Fluid Mechanics Equations

Fluid mechanics is based on three basic laws of conservation: mass, momentum, and energy. The equation for conservation of mass, also called the continuity equation,

and the equation for conservation of momentum are solved for all flowing systems. For systems with heat transfer or with compressible flow, the energy equation is included in the analysis. In addition, a species balance is performed when there are reactions included in the analysis and several turbulence models are available to be chosen by the user when the flow is turbulent.

Mass Balance

The continuity equation, valid for compressible and incompressible flow is calculated in FLUENT as follows:

$$\frac{\partial \rho}{\partial t} + \frac{\partial}{\partial x_i}(\rho u_i) = S_m$$

where ρ is the density of the fluid, t is time, u_i is velocity in the i direction, x_i is distance in the i direction, and S_m is a source term. For steady-state calculations completed in this study, $\partial \rho / \partial t = 0$ and the source term $S_m = 0$; therefore this equation can be simplified to:

$$\frac{\partial}{\partial x_i}(\rho u_i) = 0$$

In this work, the individual species densities, ρ_i' , are calculated as linear functions of temperature except for the density of titanium dioxide which is constant; and the total mixture density, ρ , is calculated using the volume-weighted-mixing-law:

$$\rho = \frac{1}{V} \sum_i \rho_i' V_i'$$

where V is the volume of the mixture and V_i' is the volume occupied by species i' .

Momentum Balance

The steady state conservation of momentum equation is calculated in FLUENT as follows:

$$\frac{\partial}{\partial x_j}(\rho u_i u_j) = -\frac{\partial p}{\partial x_i} + \frac{\partial \tau_{ij}}{\partial x_j} + \rho g_i + F_i$$

where p is the local static pressure and F_i is a general source term. To simplify the problem at hand, with high velocity low density gases, all gravitational forces, g_i , are set to zero and there are no external source terms, F_i . For a constant volume system and in rectangular coordinates, the stress tensor, τ_{ij} , is calculated in FLUENT as:

$$\tau_{ij} = \mu \left(\frac{\partial u_i}{\partial x_j} + \frac{\partial u_j}{\partial x_i} \right) \quad i \neq j$$

meaning the fluid is treated as Newtonian. μ is the viscosity of the mixture and is calculated via the mass-weighted-mixing-law:

$$\mu = \frac{1}{M} \sum_i \frac{\mu_i}{M_i}$$

where M is the mass of the fluid system and M_i is the total mass of species i in the system. In the cylindrical coordinate system, the radial component of the momentum balance can be written as follows:

$$\frac{\partial}{\partial r}(\rho u_r u_r) + \frac{\partial}{\partial \theta}(\rho u_r u_\theta) + \frac{\partial}{\partial z}(\rho u_r u_z) = -\frac{\partial p}{\partial r} + \frac{\partial \tau_{rr}}{\partial r} - \frac{\partial \tau_{r\theta}}{\partial \theta} + \frac{\partial \tau_{rz}}{\partial z}$$

Energy Balance

FLUENT solves the steady-state energy balance equation as follows:

$$\frac{\partial}{\partial x_i}(u_i(\rho E + p)) = \frac{\partial}{\partial x_i} \left(k_{\text{eff}} \frac{\partial T}{\partial x_i} - \sum_j h_i' J_j' + u_j \tau_{ij} \right) + S_h$$

$$E = h - \frac{p}{\rho} + \frac{u_i^2}{2}$$

where k_{eff} is the effective conductivity ($k + k_t$), k_t is the turbulent thermal conductivity calculated by the turbulence equations, T is temperature, J_j' is the diffusion flux of species

j' , and S_h is a general source term. The enthalpy, h , is defined for an incompressible gas as:

$$h = \sum_j m_j' h_j' + \frac{p}{\rho}$$

where m_j' is the mass fraction of species j' and h_j' is defined as:

$$h_j' = \int_{T_{ref}}^T c_{p,j}' dT$$

T_{ref} is 298.15 K and $c_{p,j}'$ is the heat capacity of species j' . Since the chemical reaction studied in this work is only slightly endothermic, $\Delta H = -22.5$ kJ/mol, a heat of reaction term, S_h , was not included in the energy balance equation to reduce computational time.

Analyses of Chloride Process Reactors

All analyses in this work have been carried out using the segregated, 3-dimensional, steady state solver in FLUENT. To use the segregated solver means that the continuity, momentum, and sometimes energy and species equations are solved in succession. Also solved in each analysis is the RNG turbulence model. The RNG model is more accurate and reliable than the standard $k-\epsilon$ model due to several added features including: an analytical formula for Prandtl numbers, and higher accuracy for lower turbulent number flows and swirling flows (Fluent Incorporated, 1998).

To perform a CFD analysis, the fluid properties must be specified in the solver. In FLUENT, the system must be initialized with a fluid filling the entire volume; and the fluid chosen cannot be one of the fluids flowing in through an inlet. It is also necessary to have the initial fluid not be one of the reactants or a relatively dense fluid causing convergence problems. The initial fluid used in this research is called nitrogen and is given the properties of oxygen. Convergence can be verified with the depletion of

nitrogen since nitrogen is not one of the inlet flowing fluids or a reaction product. Table 1 lists the fluid properties for the four species used in this research, oxygen, titanium tetrachloride, titanium dioxide, and chlorine.

Table 1 Fluid Properties (Fluent Inc.)

	Oxygen	Titanium Tetrachloride	Titanium Dioxide	Chlorine
Density (kg/m^3)	Piecewise linear	Piecewise linear	4250	Piecewise linear
Heat Capacity (J/kg-K)	919.31	560	905	650
Thermal Conductivity (W/m-K)	0.0246	0.017	0.09	0.0082
Viscosity (kg/m-s)	1.919e-5	2.2e-5	0.009	1.33e-5
Molecular Weight (kg/kgmol)	32	189.7	79.9	70.9
Standard State Enthalpy (J/kgmol)	0	-7.2086e+8	2397000	2816.454
Standard State Entropy (J/kgmol-K)	205026.9	49322	54332	222988
Reference Temperature (K)	298.15	298.15	298.15	298.15

Piecewise-linear functions of temperature are used for density for the three fluids. Table 2 lists those values.

Table 2 Density as a Function of Temperature

	Oxygen	Titanium Tetrachloride	Chlorine
Temperature (K)	300	300	300
Density (kg/m^3)	1.3	20	2.95
Temperature (K)	2000	2000	2000
Density (kg/m^3)	0.2	3	0.44

FLUENT can currently model particle flow simulations; however, the discrete phase must be initialized as an inlet boundary condition. FLUENT cannot currently model a reaction-to-particle system without a complex User Defined Function (UDF), which is currently unavailable to users. The titanium dioxide in this study was consequently modeled as a high density, low volume fluid with all the properties of the solid titanium dioxide with the exception of viscosity. Therefore, the density of titanium dioxide is modeled as a constant and not as a function of temperature.

The mixture properties must also be established by specifying which mixing law calculation is to be used for each property. For each case study, the density of the mixture is calculated using the volume-weighted-mixing-law as described earlier because titanium dioxide solid is being approximated as a fluid. Using the volume-weighted-mixing-law, as opposed to the ideal gas law, yields a more accurate approximation of the pressure profile, thus a more accurate flow profile. Thermal conductivity and viscosity are calculated using the mass-weighted-mixing-law as described earlier in this chapter. A constant total mixture diffusivity is used to facilitate convergence.

Finally, the eddy-dissipation reaction model is used in each case study. The eddy-dissipation model is ideal for near instantaneous reactions where the reaction rate is mostly dependant on the rate of mixing (Fluent Incorporated, 1998). The use of this model is necessary because a hydrocarbon combustion that significantly increases the reactor temperature is usually integrated in each reactor. FLUENT cannot perform two reaction calculations where both reactions have oxygen as a reactant and one reaction rate is oxygen-dependant (Aggus, 2000). Because of this reason, the hydrocarbon reactions

are not included and the $\text{TiCl}_4 - \text{O}_2$ reaction should not be modeled with the Arrhenius equation because the reactor temperature is too low.

All analyses are presented with the assumption that titanium dioxide can be approximated as part of the continuum fluid. To separate the titanium dioxide into a discrete phase, a UDF would be required to simulate the gas-to-solid particle reaction and would have to include the initial parameters of the solid particles such as trajectory, particle diameter, particle density, and temperature.

To perform an accurate mass balance – to achieve accurate velocity profiles – the actual density of solid titania is used in the calculations. Difficulties arise in the analyses when attempting to calculate a mixture viscosity and a mixture diffusivity. For each species in FLUENT, a fluid viscosity must be specified and used in one of the available mixing laws (i.e. mass weighted mixing law) to calculate the mixture viscosity. A relatively high value for viscosity was assumed to approximate the viscous forces on the particles. Changes in the approximated viscosity would affect the calculated pressure drop from the momentum balance.

Also approximated was the mixture diffusivity. Since the main profile of interest in the analyses is the species distribution, a constant mixture diffusivity is the most significant assumption made. Ideally for a fluid mixture, each binary diffusivity should be entered into FLUENT mixture properties. Binary diffusivities, including those of titania and various gases, can be found in reference tables or can be calculated. However, the titania is being approximated as a fluid in FLUENT, therefore the diffusion of interest is that seen by the bulk fluid and is not numerically the diffusion of gas into the solid titania particle as given in tables, but a much larger diffusion approximating the flux of

each gas species between particles. Therefore, the binary titania-gas diffusivities should be large, not small, relative to gas-gas diffusivity.

Two additional analyses were performed separately from the ones presented, one with a 50% increase in the mixture diffusivity, the other with a 50% decrease. Both analyses show little difference from each other or from the original diffusivity used. Results are presented in Appendix D.

Cabot Reactor Patent # 3,311,452

Cabot Corporation was one of the first companies to patent a TiO_2 reactor design incorporating the use of a hot gas sheathe to protect the walls from oxide scale buildup. In 1967, Cabot Corporation proposed this design specifically for the hydrolysis of TiCl_4 to TiO_2 with a hot gas sheathe protecting the yellow highlighted wall surface in Figure 8. This patent claims that no accretion occurs on the yellow highlighted wall after one week of operation when the hot combustion gas is introduced through Inlet 1 instead of through Inlet 2.

The hot gas sheathe is not the only approach used in this patent for the reduction of TiO_2 accretion. The knife-edge inlet is a widely used approach for reducing oxide scale buildup in chloride process reactors and is the large reason for the reduction of oxide scale in this reactor. The reason this method is somewhat effective is that it decreases the reactor surface area where the reactants mix and react to a single point or line. As seen in Figure 8, the red highlighted region is the knife-edge where the reactants all meet and is the point where the reaction is initialized when the combustion gases are introduced through Inlet 1.

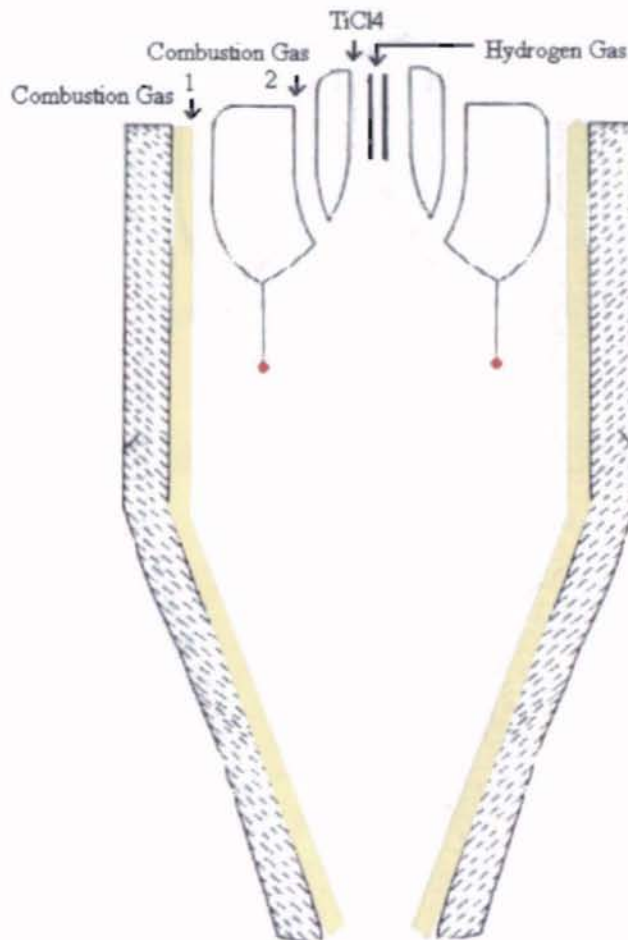


Figure 8 Cabot Reactor Specified by Patent

Since the oxidation reaction is of interest in this research, it has been used in the analyses of this reactor. Figure 9 illustrates the analyses performed with the blue highlighted region being the wall surface protected by the hot chlorine gas wall. Because the chlorine is fed between the reactants and forces the reaction to occur downstream of the inlet walls, these analyses test the effectiveness of the gas blanket alone to prevent TiO_2 accretion.

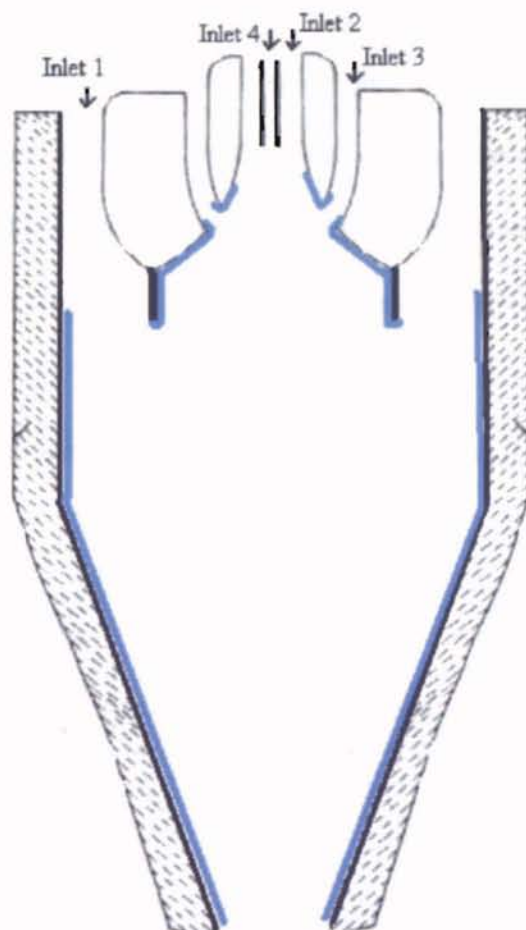


Figure 9 Cabot Reactor Analyzed

Four separate CFD analyses were performed on the Cabot reactor and include the following:

Table 3 Cabot Analyses

<p>CASE I Inlets 1 & 2: Low Momentum Chlorine Gas Inlet 3: Titanium Tetrachloride Inlet 4: Oxygen</p>	<p>CASE II Inlets 1 & 2: High Momentum Chlorine Gas Inlet 3: Titanium Tetrachloride Inlet 4: Oxygen</p>
<p>CASE III Inlets 1 & 2: Low Momentum Chlorine Gas Inlet 3: Oxygen Inlet 4: Titanium Tetrachloride</p>	<p>CASE IV Inlets 1 & 2: High Momentum Chlorine Gas Inlet 3: Oxygen Inlet 4: Titanium Tetrachloride</p>

The locations of the titanium tetrachloride and oxygen inlets were exchanged to evaluate the effect it would have on the rate of mixing. For each scenario, Inlets 1 and 3 remain the inflows for the hot chlorine gas, which is fed at either a lower flow rate or a higher flow rate causing the momentum of the chlorine to be equal to the momentum of the oxygen gas.

The three-dimensional drawing of the Cabot reactor is shown in Figure 10.

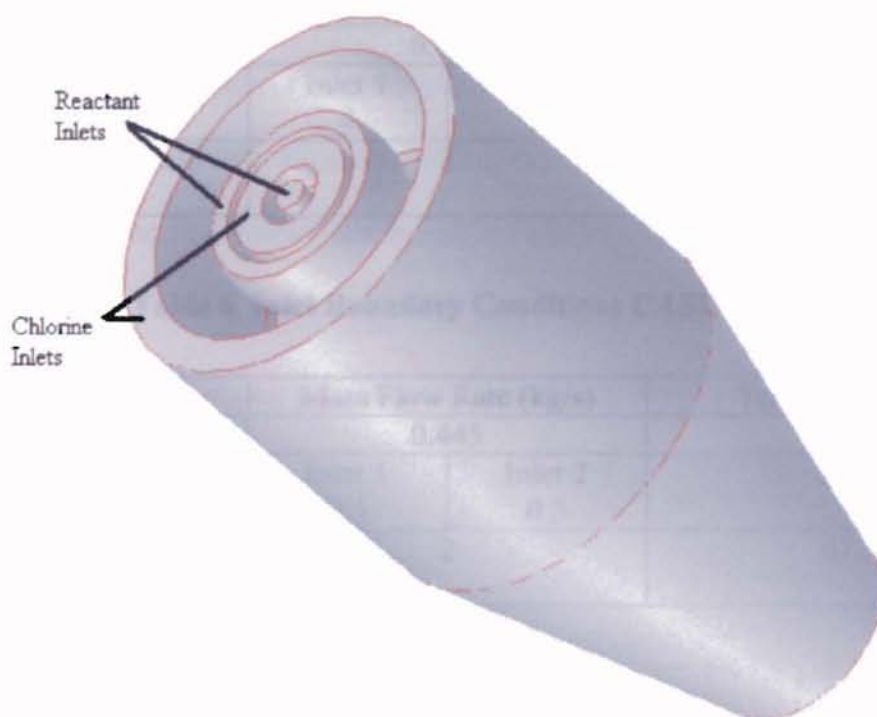


Figure 10 3-D Cabot Reactor

The inlet flow conditions normal to the inlet boundary face for each case study are given in the following tables.

Table 4 Inlet Boundary Conditions CASE I

	Mass Flow Rate (kg/s)		Temperature (K)
Oxygen (Inlet 4)	0.445		1228
Chlorine	Inlet 1 0.5	Inlet 2 0.5	1228
Titanium Tetrachloride (Inlet 3)	2		672

Table 5 Inlet Boundary Conditions CASE II

	Mass Flow Rate (kg/s)		Temperature (K)
Oxygen (Inlet 4)	0.445		1228
Chlorine	Inlet 1 4	Inlet 2 1.5	1228
Titanium Tetrachloride (Inlet 3)	2		672

Table 6 Inlet Boundary Conditions CASE III

	Mass Flow Rate (kg/s)		Temperature (K)
Oxygen (Inlet 3)	0.445		1228
Chlorine	Inlet 1 0.5	Inlet 2 0.5	1228
Titanium Tetrachloride (Inlet 4)	2		672

Table 7 Inlet Boundary Conditions CASE IV

	Mass Flow Rate (kg/s)		Temperature (K)
Oxygen (Inlet 3)	0.445		1228
Chlorine	Inlet 1 4	Inlet 2 1.5	1228
Titanium Tetrachloride (Inlet 4)	2		672

PPG Industries Reactor Patent # 3,586,055

PPG Industries, Inc. patented a reactor design in 1971 that used a chlorine gas stream to separate the reactants at the combustion chamber entrance and to keep reaction from occurring on the inlet surfaces. Wilson's main claim involved plates that serve to distribute flow into the combustion chamber more evenly and thus reduce scale growth. Since including the distributor plates is a difficult CAD task and causes severe convergence problems due to very small mesh volumes, the distributor plates are omitted from this analysis. The claim that severe scale occurs in this reactor without the use of the distributor plates regardless of the use of a chlorine gas sheath is analyzed. This reactor is designed specifically for the oxidation of titanium tetrachloride. A solid and a wireframe view of the PPG reactor are shown in Figure 11 and Figure 12, respectively.

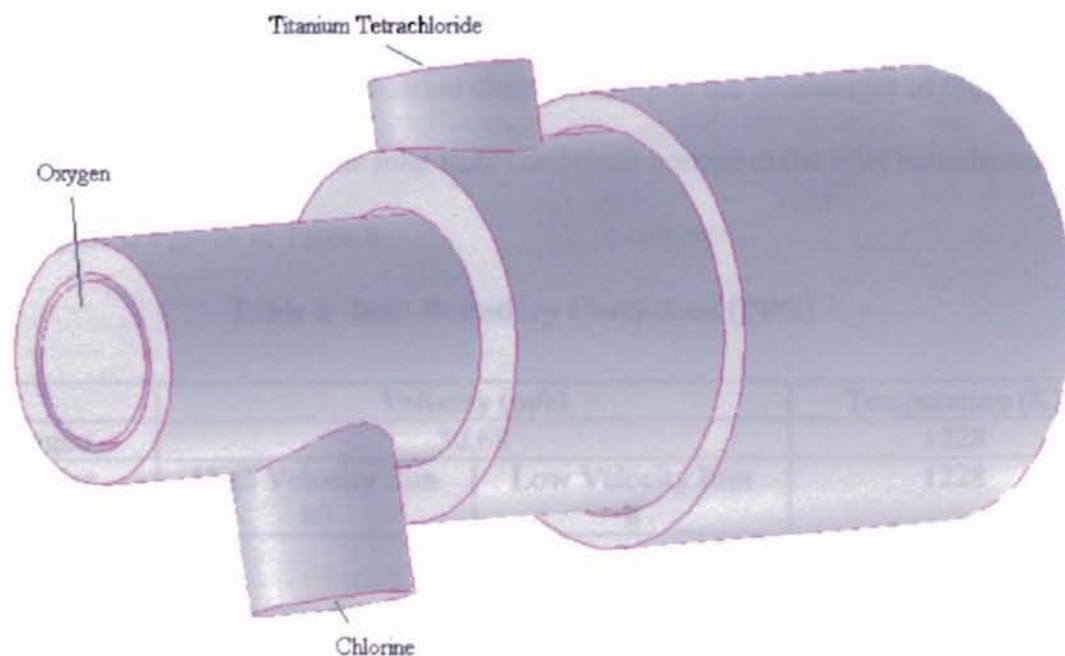


Figure 11 PPG Reactor (Solid View)

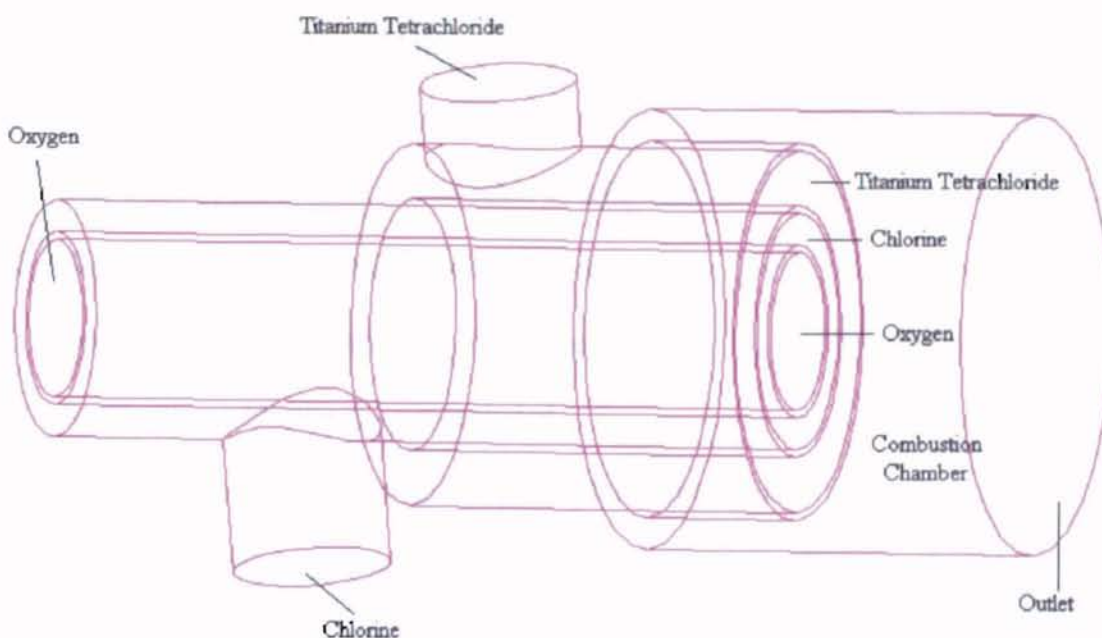


Figure 12 PPG Reactor (Wireframe View)

Two analyses were performed on this reactor, one with a low relative chlorine flow rate, and another with a chlorine flow rate causing the momentum of the oxygen stream at the entrance of the combustion chamber to equal the momentum of the chlorine stream at the same location. The inlet flow conditions normal to the inlet boundaries for both analyses are given in Table 8.

Table 8 Inlet Boundary Conditions (PPG)

	Velocity (m/s)		Temperature (K)
Oxygen	50.68		1228
Chlorine	High Velocity Run 80	Low Velocity Run 8	1228
Titanium Tetrachloride	20		672

Kerr-McGee Corporation Reactor

A simplified model of Kerr-McGee's chloride process reactor was analyzed. Several simplifying assumptions include:

1. The walls of the reactor are modeled as adiabatic.
2. The hydrocarbon reaction is not included.
3. Propane and sand are not included in the analysis.
4. Rutilization additives are not included.
5. The titanium dioxide is modeled as a high-density fluid.

The three-dimensional geometry of the Kerr-McGee reactor drawn in the CAD software included with the FLUENT package, Gambit, is illustrated below from two perspectives.

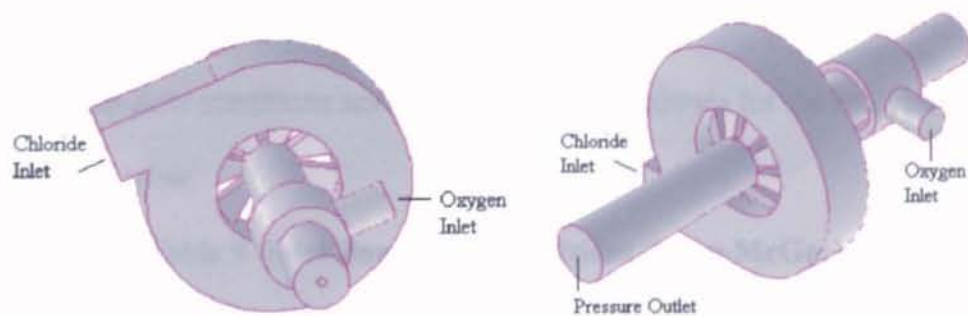


Figure 13 Solid KM Reactor (Front and Rear View)

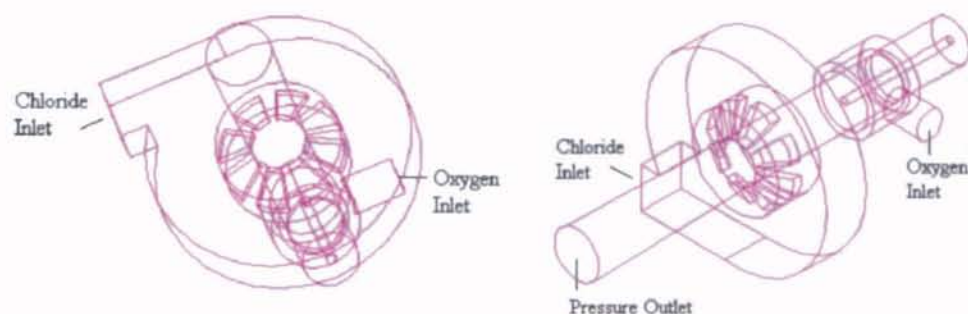


Figure 14 Wire Frame KM Reactor (Front and Rear View)

The geometry includes two velocity inlets for the reactants and a pressure outlet boundary condition set to 0 psig. The long thin tube at the front of the reactor is the inlet nozzle for the propane/sand mixture and is treated as an adiabatic wall in this analysis. The oxygen and chloride inlet spools are designed to provide an evenly distributed flow of reactants into the reactor. The eight discrete chloride nozzles are designed to provide for enhanced mixing and faster reaction of reactants.

The inlet flow conditions normal to the inlet boundaries for the analysis are given in the following table.

Table 9 Inlet Boundary Conditions (Kerr-McGee)

	Velocity (m/s)	Temperature (K)
Oxygen	82.3	1228
Titanium Tetrachloride	6.3	672

These velocities were set to match the inlet mass flow rates and temperatures given by Kerr-McGee.

Altered Kerr-McGee Reactor with Gas Blanket

The purpose of the gas-blanket tactic is to keep both reactants from contacting any point on the reactor surface simultaneously and reacting thereon. The gas-blanket should also prevent developing titanium dioxide particles from migrating to the surface.

An additional analysis has been performed on the Kerr-McGee reactor presented above, now with a hot chlorine gas stream injected immediately upstream of and adjacent to the eight titanium tetrachloride nozzles. The chlorine is fed into the reactor concentrically at a sixty-degree angle parallel to the chloride nozzles. Illustrations of only the chlorine and TiCl_4 inlets are presented below from several perspectives.

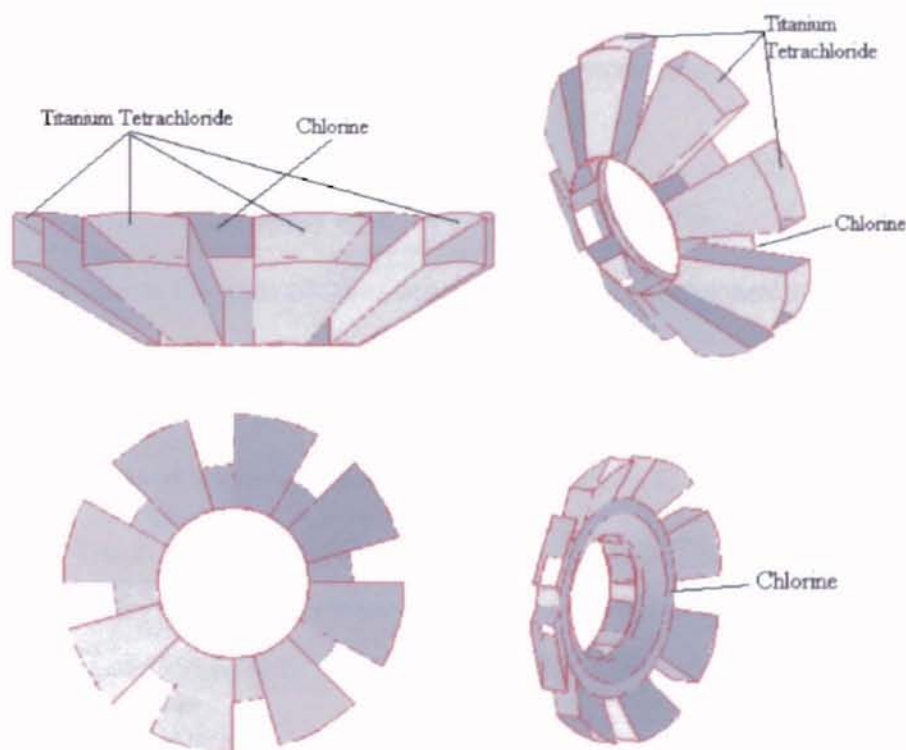


Figure 15 Chloride and Chlorine Inlets of Gas-Blanketed KM Reactor

The boundary conditions for this analysis are identical to the previous Kerr-McGee analysis with the exception of the additional chlorine inlet. The chlorine is fed at

a flow rate of 53 m/s for the momentum of the chlorine stream at the reactor entrance to equal the momentum of the oxygen stream.

Summary

This chapter discussed four chloride process reactor systems that were analyzed using computational fluid dynamics software, FLUENT, and the continuity, momentum, and energy equations used to perform the analyses. Two of the reactor systems were patented gas-blanketed reactors that claim to reduce TiO_2 accretion using the gas layer. The third and fourth analyses are on Kerr-McGee's current reactor both without and with an added gas layer to separate the inflowing reactants to meet concurrently at the reactor walls.

CHAPTER IV

RESULTS OF CFD ANALYSES

Introduction

This chapter discusses the results obtained by analyzing the four chloride process reactors discussed in the previous chapter. The analyses are aimed at determining the efficacy of a chlorine gas blanket to reduce oxide accretion at the reactor walls by examining the walls for both titanium dioxide and an oxygen/chloride mixture. Also, the effect of the gas blanket on mixing is examined by determining the total mass of titanium dioxide exiting the reactors.

Cabot Reactor Patent # 3,311,452

As detailed in Chapter III, four separate runs were performed on the Cabot reactor design.

<p style="text-align: center;">CASE I</p> <p style="text-align: center;">Inlets 1 & 2: Low Momentum Chlorine Gas</p> <p style="text-align: center;">Inlet 3: Titanium Tetrachloride</p> <p style="text-align: center;">Inlet 4: Oxygen</p>	<p style="text-align: center;">CASE II</p> <p style="text-align: center;">Inlets 1 & 2: High Momentum Chlorine Gas</p> <p style="text-align: center;">Inlet 3: Titanium Tetrachloride</p> <p style="text-align: center;">Inlet 4: Oxygen</p>
<p style="text-align: center;">CASE III</p> <p style="text-align: center;">Inlets 1 & 2: Low Momentum Chlorine Gas</p> <p style="text-align: center;">Inlet 3: Oxygen</p> <p style="text-align: center;">Inlet 4: Titanium Tetrachloride</p>	<p style="text-align: center;">CASE IV</p> <p style="text-align: center;">Inlets 1 & 2: High Momentum Chlorine Gas</p> <p style="text-align: center;">Inlet 3: Oxygen</p> <p style="text-align: center;">Inlet 4: Titanium Tetrachloride</p>

Inlet numbers are presented in Figure 16.

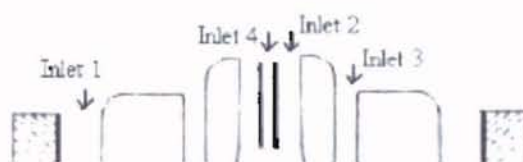


Figure 16 Cabot Reactor, Inlet Configuration

In Case I, chlorine gas is fed to the reactor at a low flow rate relative to the flow rates of the reactants. The chlorine gas is not expected to provide an effective gas sheath to prevent oxide deposition. The following figures show mole fractions of oxygen, titanium tetrachloride, chlorine, and titanium dioxide in a two-dimensional, vertical, longitudinal slice of the reactor. Mole fraction is defined as the number of moles of species i divided by the total number of moles in the system.

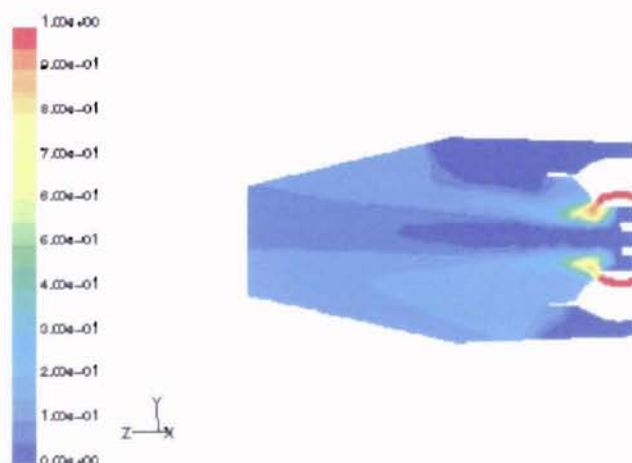


Figure 17 (Cabot Case I) Mole Fraction O_2

Figure 17 shows the oxygen exiting the inlet nozzle and expanding around the surfaces adjacent to the inlet due to the sudden pressure drop highlighted in the following figure.

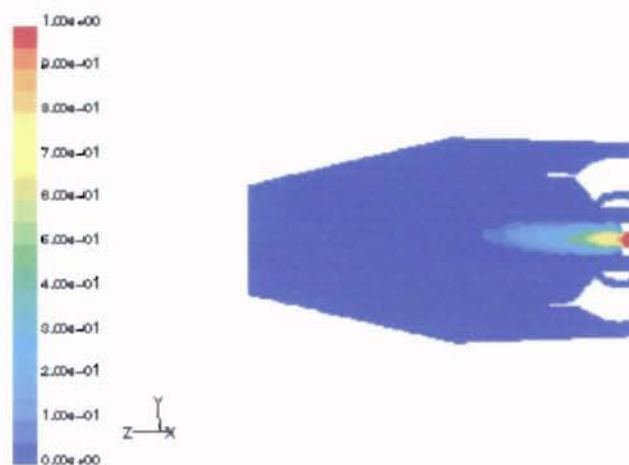


Figure 18 (Cabot Case I) Mole Fraction TiCl_4

It can be seen from Figure 17 and Figure 18 that a mixture of oxygen and titanium tetrachloride does not exist on any surface in the reactor. The wall surface surrounding the titanium tetrachloride inlet is dark blue in the oxygen concentration profile and vice versa.

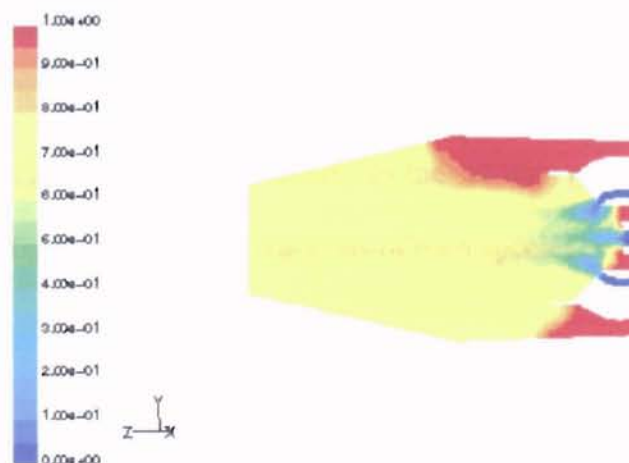


Figure 19 (Cabot Case I) Mole Fraction Cl_2

Figure 19 shows that chlorine does not overcome the flow of oxygen and titanium tetrachloride and does not coat most walls of the reactor.

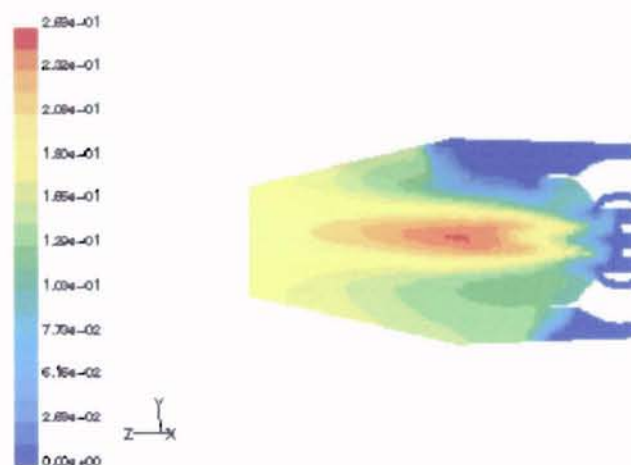


Figure 20 (Cabot Case I) Mole Fraction TiO_2

Figure 20 shows titanium dioxide just upstream of the north wall of the oxygen inlet and along the diverging wall just downstream of the oxygen inlet. The titanium dioxide may also be starting to plug the outer chlorine inlet.

Case II is identical to Case I except with an increase in chlorine gas flow rate. The flow rate is set so that the momentum of the chlorine gas equals that of the oxygen. The following figures show mole fractions of each species.

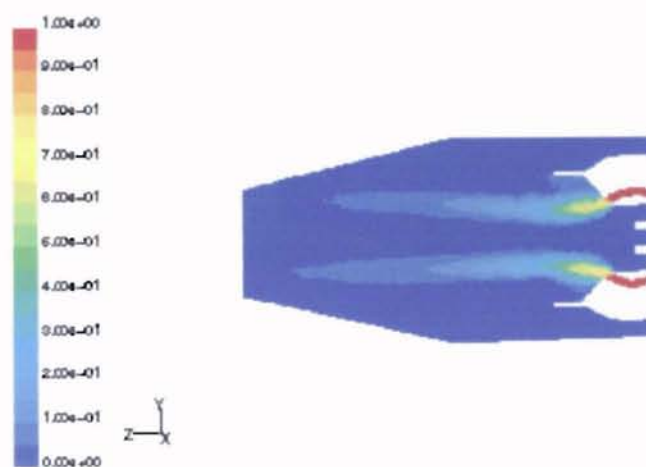


Figure 21 (Cabot Case II) Mole Fraction O_2

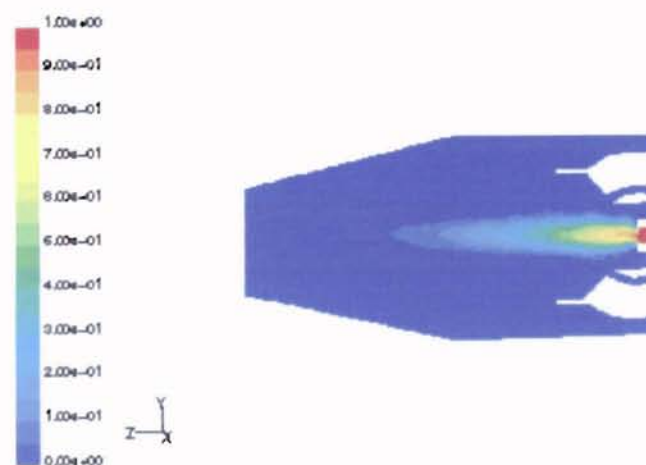


Figure 22 (Cabot Case II) Mole Fraction $TiCl_4$

Figure 21 and Figure 22 show that a mixture of oxygen and titanium tetrachloride does not exist on any reactor surface; therefore, accretion is not initiated by surface reaction on the reactor walls.

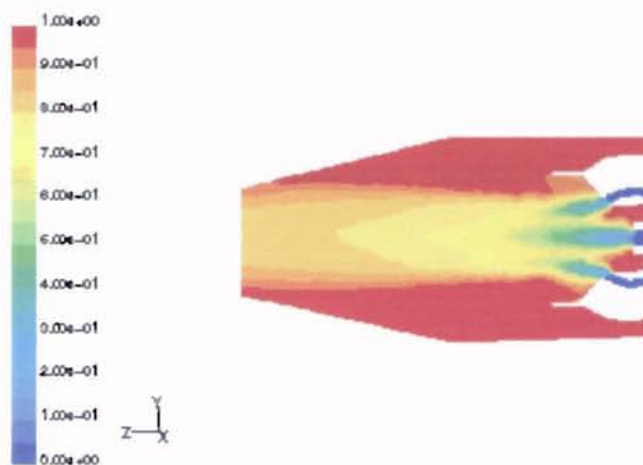


Figure 23 (Cabot Case II) Mole Fraction Cl_2

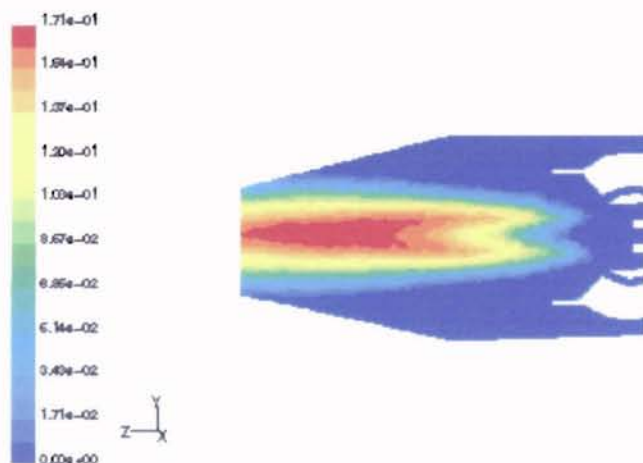


Figure 24 (Cabot Case II) Mole Fraction TiO_2

With the hot chlorine gas sheathe, the titanium dioxide does not migrate to the surfaces surrounding the reactant inlets as illustrated in Figure 24. Shown in dark blue, there is a zero mole fraction of titanium dioxide near the surfaces of the reactor surrounding the reactant inlets.

Case III analysis is run to determine the optimum locations of the reactant inlets. Case III is identical to Case I, except the positions of the oxygen and chloride inlets are exchanged. The following figures show mole fractions of each species.

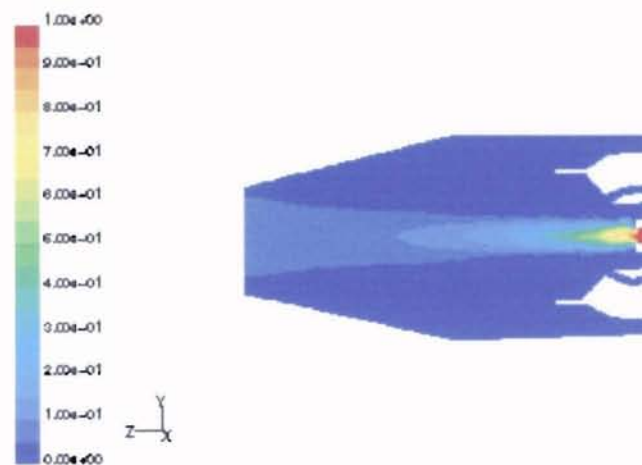


Figure 25 (Cabot Case III) Mole Fraction O_2

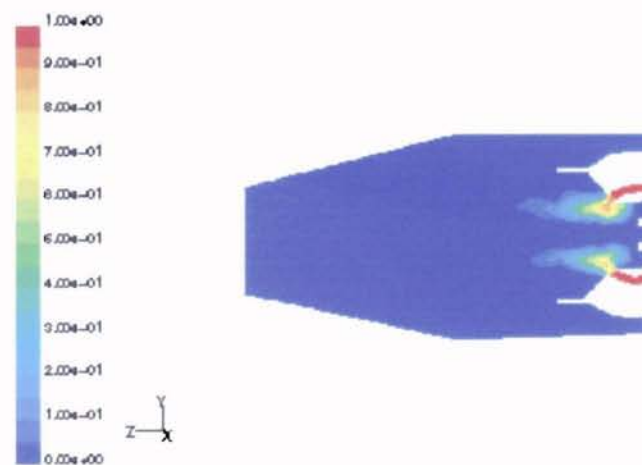


Figure 26 (Cabot Case III) Mole Fraction $TiCl_4$

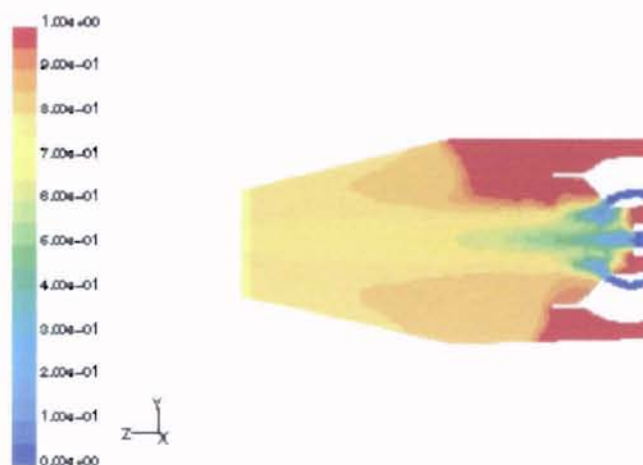


Figure 27 (Cabot Case III) Mole Fraction Cl_2

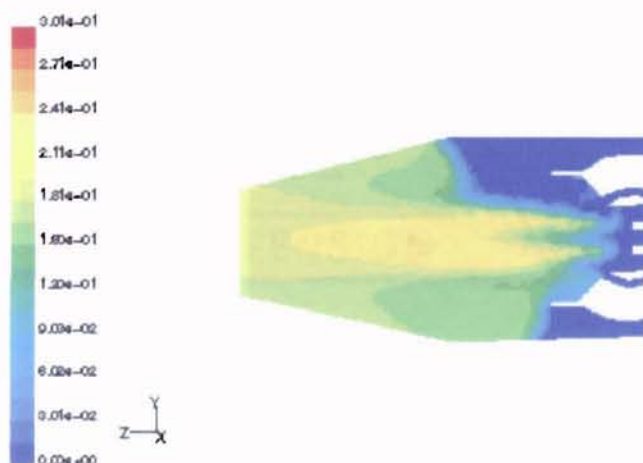


Figure 28 (Cabot Case III) Mole Fraction TiO_2

The results of Case III are similar to Case I in that the reactants do not co-exist on any surface of the reactor due to the reactor design; however, the titanium dioxide freely migrates to the reactor walls.

Case IV, like Case II, incorporates an increased chlorine flow rate. The following figures illustrate species mole fractions.

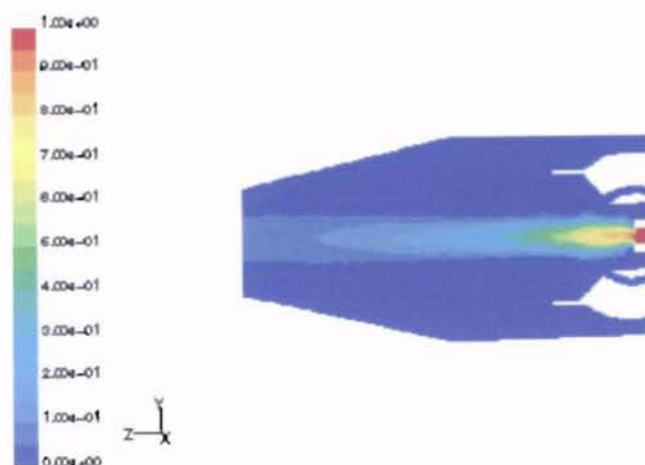


Figure 29 (Cabot Case IV) Mole Fraction O_2

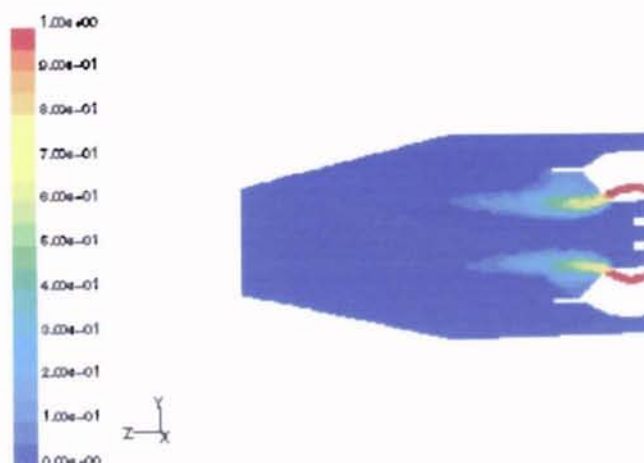


Figure 30 (Cabot Case IV) Mole Fraction $TiCl_4$

As in each of the other Cabot analyses, Figure 29 and Figure 30 show in the dark blue, zero mole fraction regions, that oxygen and titanium tetrachloride do not coexist on any reactor wall.

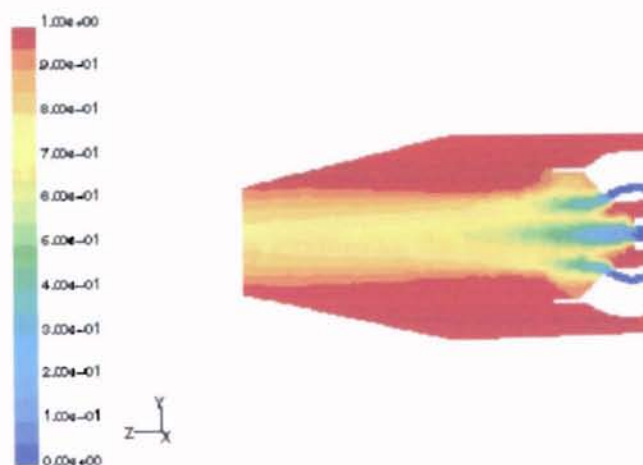


Figure 31 (Cabot Case IV) Mole Fraction Cl_2

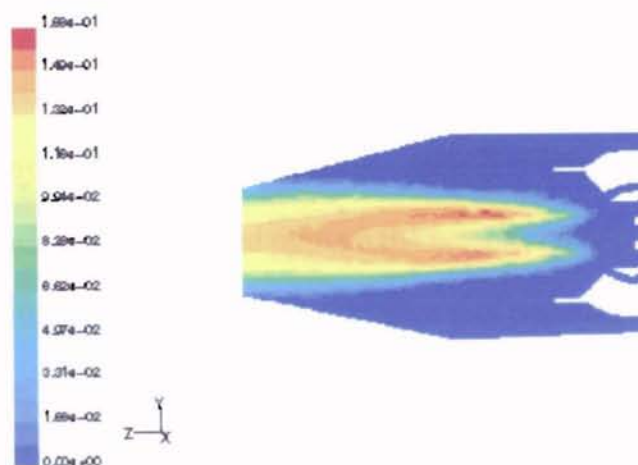


Figure 32 (Cabot Case IV) Mole Fraction TiO_2

The chlorine gas layer in Case IV, as in Case II forces the reaction to occur downstream of the inlet nozzle walls and prevents titanium dioxide from migrating to the reactor walls near the inlet surfaces.

The very low flow rates/pressures of the chlorine gas streams in Cases I and III cause the analyses to be very susceptible to deviations from symmetry due to the

asymmetric mesh. For example, average mesh volumes may be slightly larger on one side of the reactor.

Because the inlet flow rates and the rate of reaction are identical in each case, the rate of mixing can be evaluated by examining the mass flow rate of titanium dioxide exiting the reactor. The following table illustrates these results.

Table 10 Cabot Reactor TiO_2 Flow Rates

Case I	0.730 kg/s TiO_2
Case II	0.830 kg/s TiO_2
Case III	0.718 kg/s TiO_2
Case IV	0.833 kg/s TiO_2

This table shows that for Cases I and III, when the chlorine gas is fed at a low flow rate, the setup with the chloride fed through the inner nozzle provides for slightly better reactant mixing. For Cases II and IV, when the chlorine gas is fed at a high flow rate, the setup with the oxygen fed through the inner nozzle gives better mixing. In both setups, feeding the chlorine in at the higher flow rate provides for a significantly higher yield of titanium dioxide.

PPG Industries Reactor Patent # 3,586,055

In the PPG reactor design, the reactants are intended to be fed concentrically to the reaction zone. The patent proposes distributor plates, which should distribute flow into the combustion chamber more evenly and thus reduce scale growth. The following results show the flow conditions for the PPG reactor prior to the proposed distributor plates.

The results from the analysis performed with a low chlorine gas flow rate are presented below as Case I. The two-dimensional contours of species mole fraction are presented to illustrate where in the reactor each chemical species is flowing.

Figure 33 and Figure 34 show the mole fractions of oxygen and titanium tetrachloride, respectively. It can be seen from Figure 34 that the momentum of the chloride, once injected into the concentric annulus, carries the gas to the opposite side of the tube. The chlorine gas, shown in Figure 35 behaves in the same way, building up on the opposite side of the chlorine inlet. The resultant pressure differential causes the fluids to flow into the combustion chamber unevenly resulting in significant backflow of the chlorine into the titanium annulus as shown in Figure 35 and of the oxide into the chlorine annulus as shown in Figure 36.

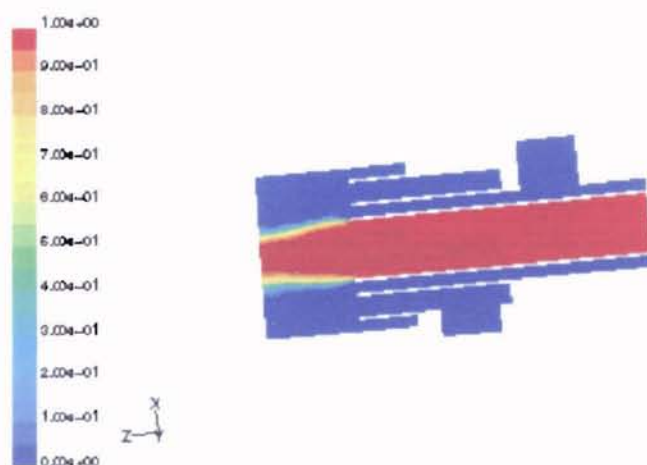


Figure 33 (PPG Reactor Case I) Mole Fraction O_2

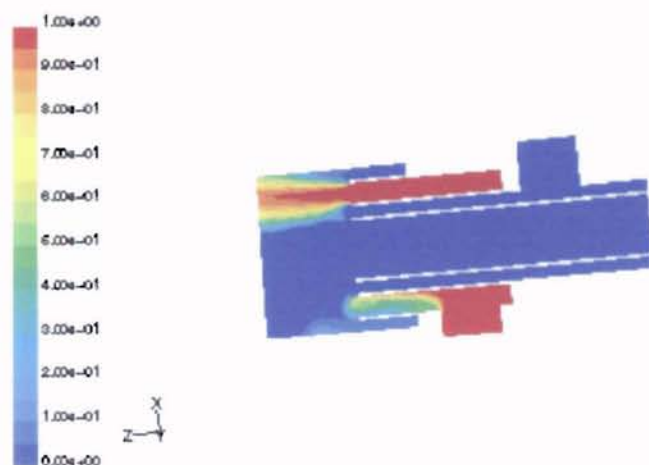


Figure 34 (PPG Reactor Case I) Mole Fraction TiCl_4

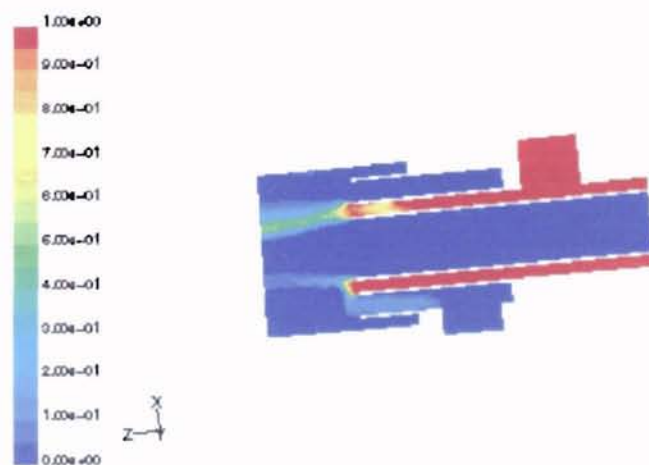


Figure 35 (PPG Reactor Case I) Mole Fraction Cl_2

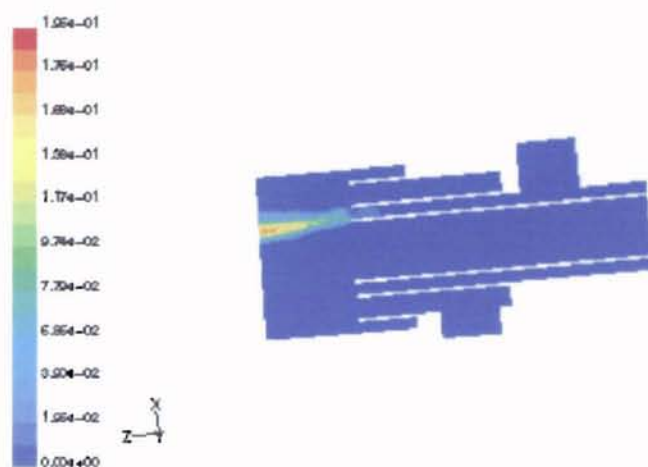


Figure 36 (PPG Reactor Case I) Mole Fraction TiO_2

From Figure 36, the titanium dioxide is residing on the reactor wall and in the chlorine gas delivery annulus where there is a light blue, non-zero mole fraction color. These results confirm that this reactor configuration would immediately accrue oxide scale that would obstruct flow.

To determine the impact of the chlorine gas blanket on oxide accretion, an additional analysis on the PPG reactor was made with an increased chlorine gas flow rate. The results of this analysis are presented below as Case II.

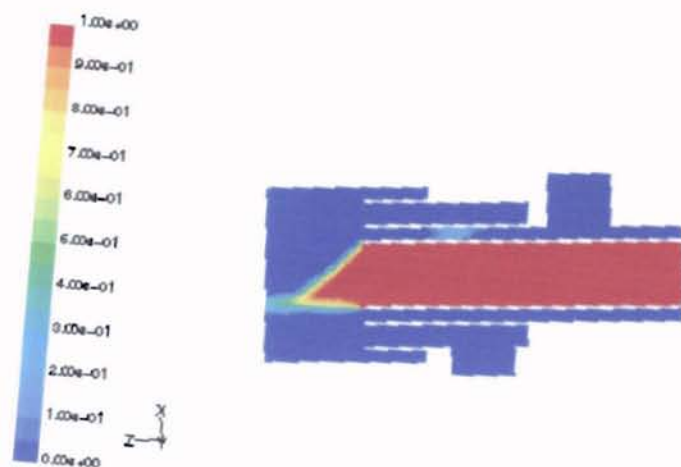


Figure 37 (PPG Reactor Case II) Mole Fraction O_2

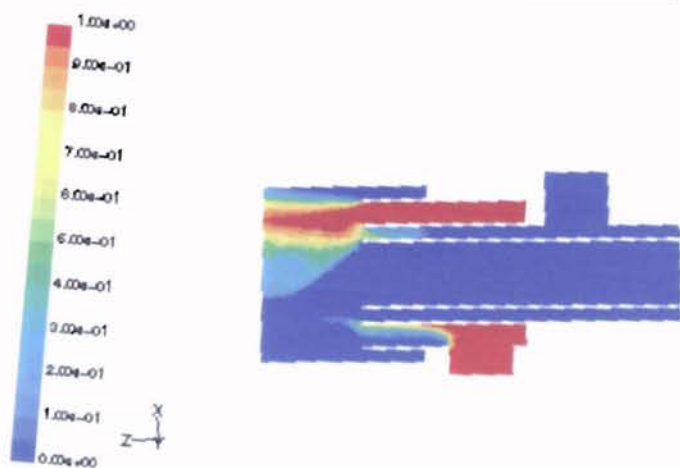


Figure 38 (PPG Reactor Case II) Mole Fraction $TiCl_4$

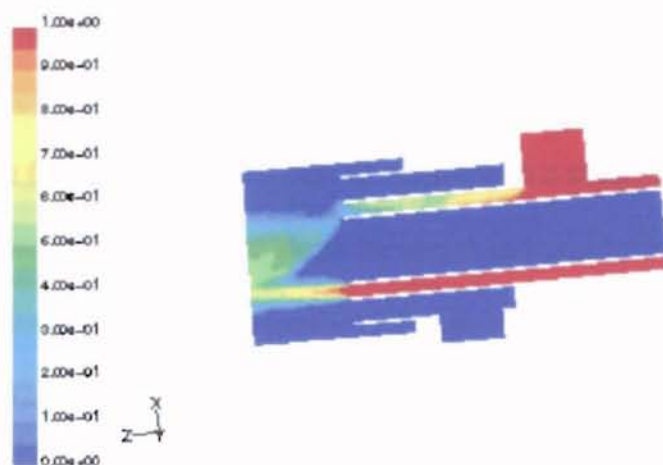


Figure 39 (PPG Reactor Case II) Mole Fraction Cl_2

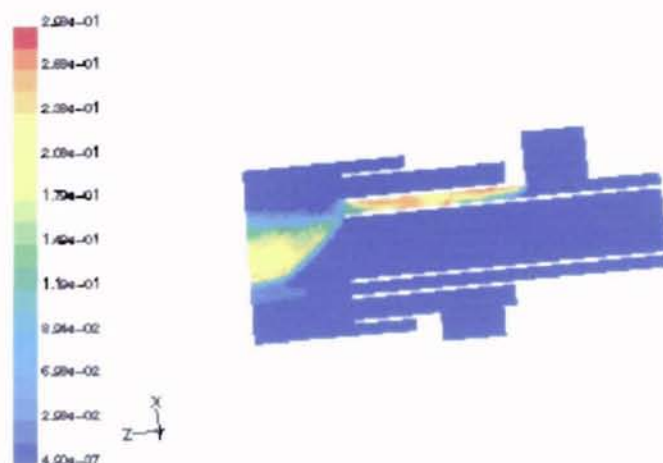


Figure 40 (PPG Reactor Case II) Mole Fraction TiO_2

Figure 37 through Figure 40 show backflow of oxygen, titanium tetrachloride, and especially titanium dioxide in the chlorine annulus. The increase of chlorine gas flow rate intensified the effect seen in Case I with the inlet chlorine gas carried to the side of the annulus opposite to the inlet boundary. Without deflector plates, increasing the chlorine gas flow rate increases the inclination of this reactor design to become plugged with oxide scale.

Kerr-McGee Corporation Reactor

The following figures compare the flow profiles of the analyzed Kerr-McGee reactor with the flow profiles of the altered reactor with a chlorine gas inlet. First, two-dimensional concentration profiles along the length of the reactor are presented followed by two-dimensional concentration profiles through the chloride inlets as shown in Figure 41 and Figure 42, respectively.

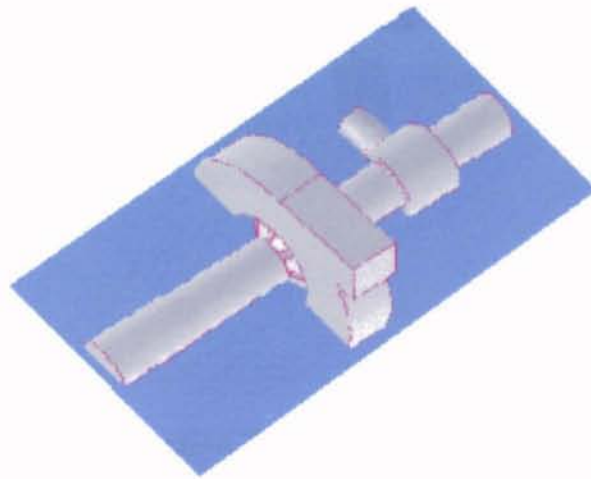


Figure 41 KM Reactor Longitudinal 2-D Rendering

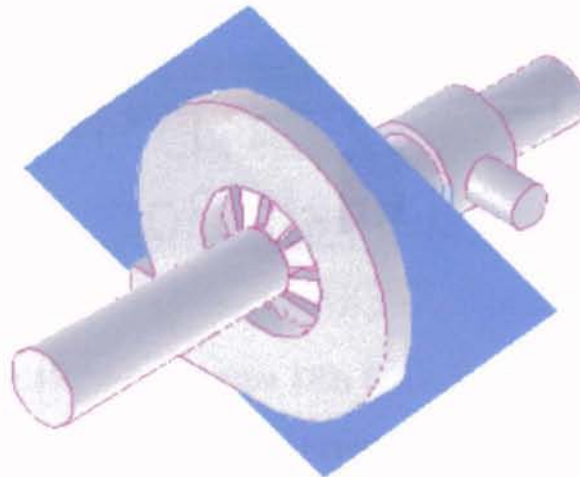


Figure 42 KM Reactor 2-D Rendering

Following are pictures of TiO_2 mole fraction taken in a longitudinal slice plane, original and altered, respectively.

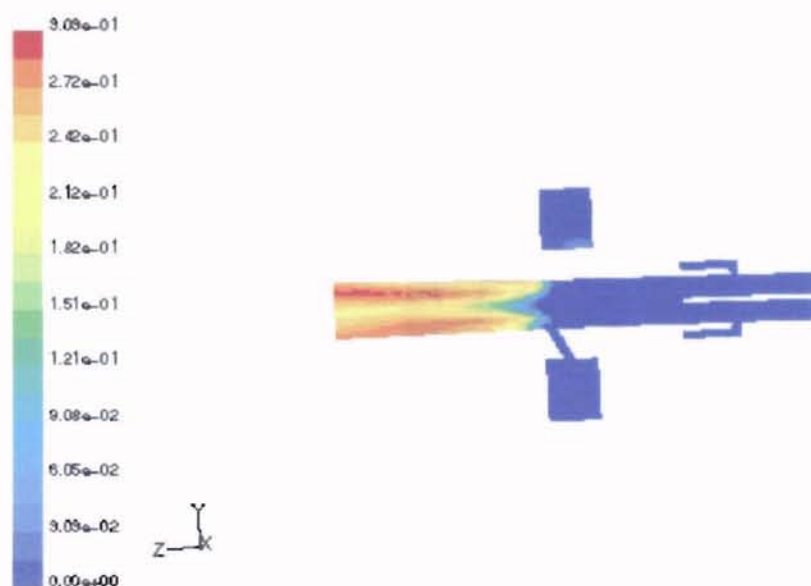


Figure 43 Mole Fraction TiO_2 (KM Reactor-Longitudinal)

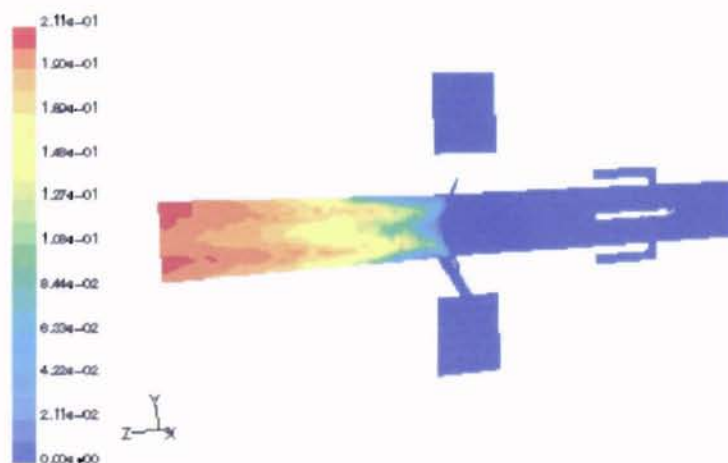


Figure 44 Mole Fraction TiO_2 (Altered KM Reactor-Longitudinal)

Figure 43 and Figure 44 show a slight improvement over the current KM reactor with regards to oxide near the wall. The addition of a chlorine gas-blanket just before the

chloride injectors seems to cause an improvement in reducing oxide accretion on the reactor walls downstream of the chloride inlets. However, a closer look at the chloride inlet walls is required.

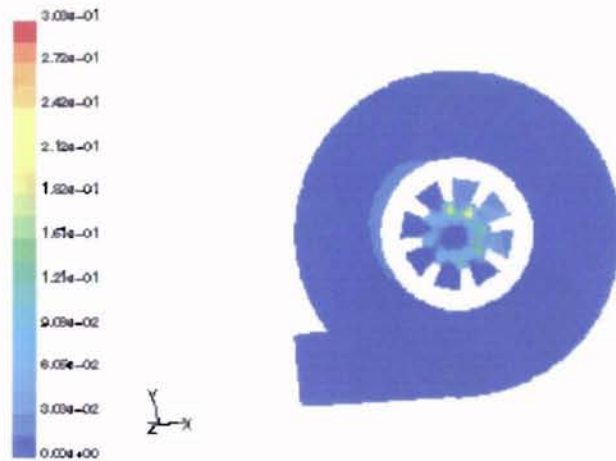


Figure 45 Mole Fraction TiO_2 (KM Reactor)

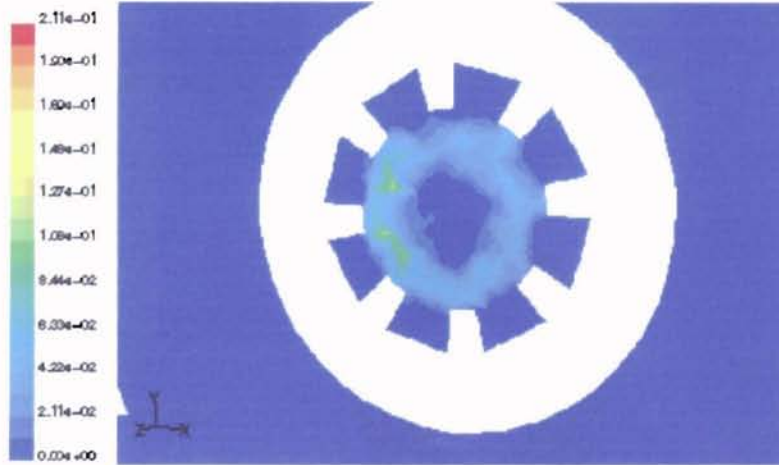


Figure 46 Mole Fraction TiO_2 (Altered KM Reactor)

The previous two illustrations present the titanium dioxide mole fraction in a slice plane through the chloride inlets, original and altered, respectively. The original KM reactor shows minute titanium dioxide in the chloride spool and nozzles possibly due to

meshing difficulty and/or low convergence. However, it can be clearly seen from the second figure that the titanium dioxide is still on seven of the eight reactor walls between the chloride nozzles.

Also important are reactant gas concentrations near the wall. The following illustrations of oxygen and titanium tetrachloride are for the original KM reactor.



Figure 47 Mole Fraction O_2 (KM Reactor)



Figure 48 Mole Fraction $TiCl_4$ (KM Reactor)

The previous figures show large concentrations of both titanium tetrachloride and oxygen on the reactor walls between the chloride nozzles. Oxygen and titanium tetrachloride coexist on the walls between the chloride nozzles in nearly stoichiometric amounts.

The following figures show gas concentrations in the same x-y plane for the gas-blanketed KM reactor.

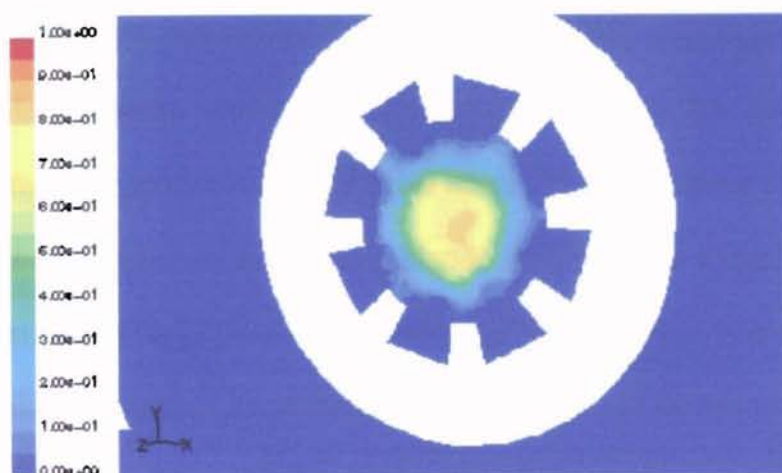


Figure 49 Mole Fraction O₂ (Altered KM Reactor)

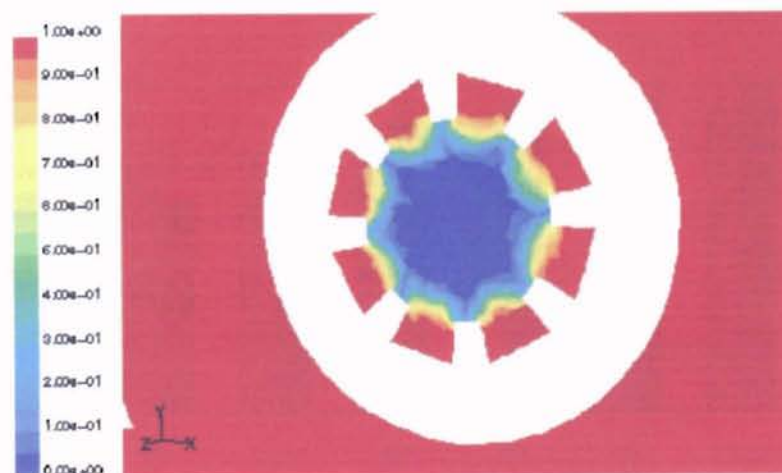


Figure 50 Mole Fraction TiCl₄ (Altered KM Reactor)

Figure 49 shows oxygen removed from four of the eight reactor walls between the chloride nozzles. Compared with Figure 47, Figure 49 shows a significant decrease in the amount of oxygen at the walls. The coexistence of oxygen and titanium tetrachloride on the walls shown in Figure 49 and Figure 50 contribute to the oxide at the walls shown in Figure 46.

Since the mixing controlled reaction rate is used in the analysis, the mixing rate can be extrapolated by the rate of production of TiO_2 . The following figure compares the original Kerr-McGee reactor with the altered version in total mass flow rate of TiO_2 through seven faces downstream of the chloride inlets. The chart shows a decrease in TiO_2 production for the first 30 cm past the chloride inlets and then a significant increase in the last 40 cm. Since the chlorine stream serves to hinder reaction near the chloride inlets and to drive the reactants away from the reactor walls, the mixing rate is reduced for the first 30 cm in the altered reactor and then the mixing is increased due to higher turbulence caused by a higher mixture density because more fluid is being fed through the reactor per unit time.

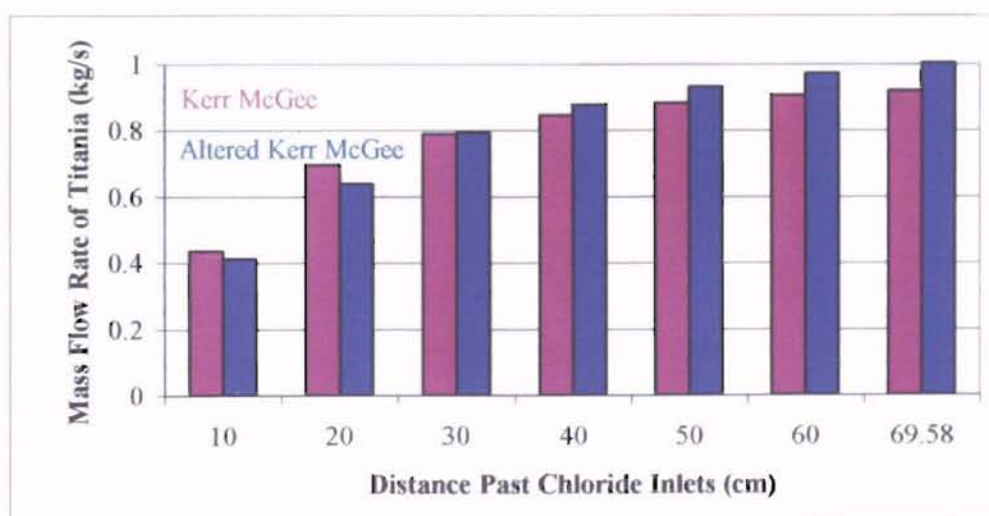


Figure 51 TiO_2 Flow Rates vs. Distance Downstream Reactor

The TiO_2 mole fraction profiles for the seven faces presented in this chart are illustrated below for both reactors.

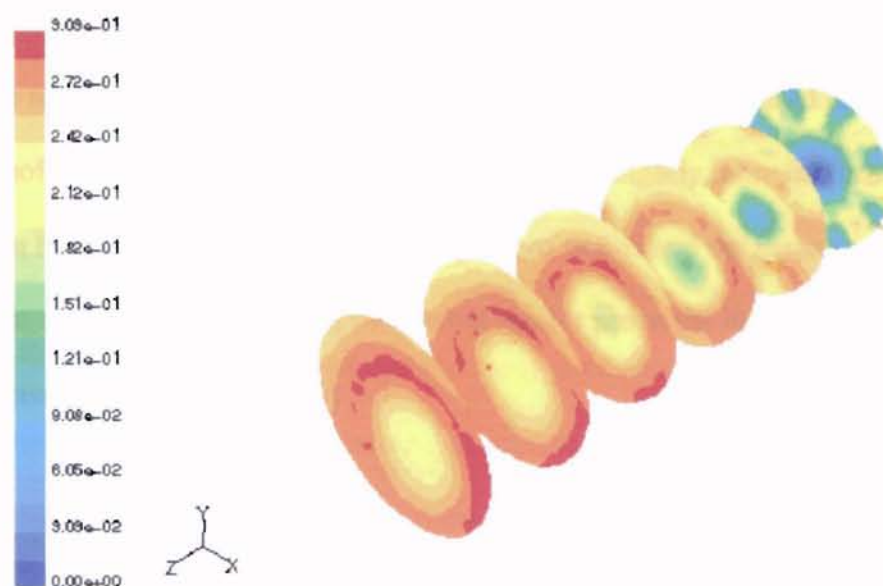


Figure 52 TiO_2 Mole Fraction in Downstream Reactor (Kerr-McGee)

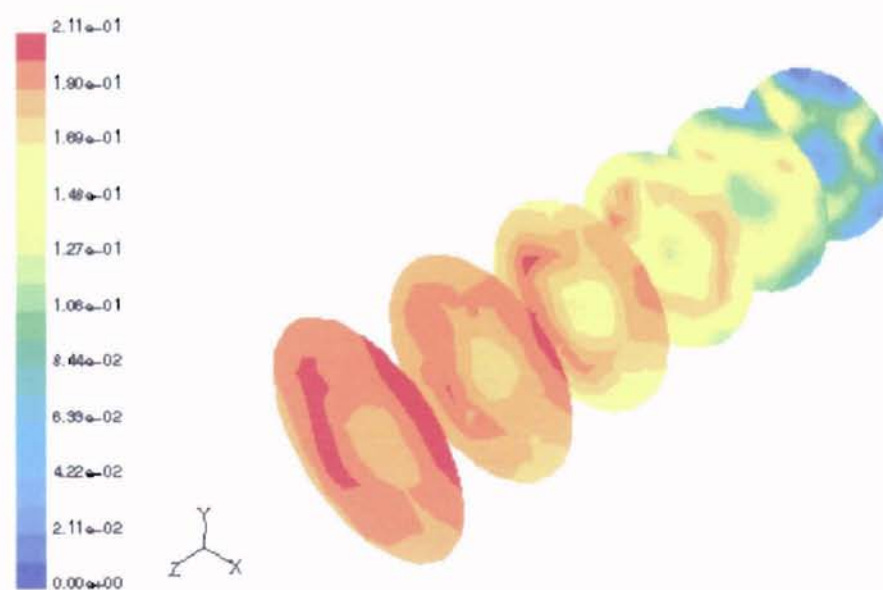


Figure 53 TiO_2 Mole Fraction in Downstream Reactor (Altered Kerr-McGee)

Figure 52 and Figure 53 show that there is a narrower distribution of TiO_2 concentration per face in the altered Kerr-McGee reactor. The color scale on the left side of Figure 52 and Figure 53 show that mole fraction range of titania for the original Kerr-McGee reactor is 0.00-3.09 (mol/mol) while the range for the altered reactor is 0.00-2.11 (mol/mol). In addition, each face in Figure 54 has a slightly more uniform color than those in Figure 53. The increase in total yield of titania and the narrower and more uniform concentration profile of the altered reactor prove the increased rate of mixing in the altered Kerr-McGee reactor.

CHAPTER V

CONCLUSIONS AND RECOMMENDATIONS

Hot gas wall sheathing is a method used frequently to reduce oxide scale on commercial reactor walls. Two patents using this method, the commercial reactor in use by Kerr-McGee, and an altered Kerr-McGee incorporating a gas sheath were each evaluated in FLUENT, a finite volume analysis software. These analyses were performed to determine the efficacy of the chlorine gas blanket to reduce oxide buildup in said reactors. This method, if effective, may contribute to eliminate the 250 lbs/hr of sand Kerr-McGee currently injects into the reactor to prevent scale buildup.

Cabot Reactor Patent # 3,311,452

The results on the four analyses performed on the Cabot reactor design show that with a very small chlorine gas flow rate, the design of the reactor is such that the reactants, oxygen and titanium tetrachloride, will not coexist on any surface in the reactor thereby initiating surface reaction on the reactor wall. However, hot titanium dioxide does migrate to most reactor surfaces in both analyses with a low chlorine gas flow rate. With a chlorine gas flow rate equalizing the momentum of the chlorine stream with the momentum of the oxygen stream at the entrance point, all titanium dioxide is swept far away from the walls of the reactor. Turbulence and mixing are significantly increased. Between the two analyses with a high chlorine gas flow rate, CASE IV, with the titanium tetrachloride delivered axially and the oxygen delivered radially downstream of the chloride inlet gives a higher mixing rate thus a greater TiO_2 yield at the outlet plane.

PPG Industries Reactor Patent # 3,586,055

Analyses of the PPG Industries reactor design verifies the patent claim that without distributor plates, chlorine and titanium tetrachloride gases fed to the reactor form a high pressure zone in the concentric annuli opposite the side of the gas inlets. The gases are then fed unevenly into the reaction zone causing severe backflow and uneven mixing in the reaction zone. Increasing the chlorine flow rate to equalize the momentum of the chlorine gas to the momentum of the oxygen stream intensifies the problem as the pressure gradient across the chlorine annulus is increased thereby causing a more uneven flow field in the reaction chamber. Without the addition of a design change, such as the addition of distributor plates, the chlorine gas sheath is not a viable method of preventing oxide deposition in this reactor.

Kerr-McGee Reactor

Kerr-McGee currently maintains continuous operation of their chloride process reactors by injecting a scouring agent into the reactor to prevent scale buildup. The Kerr-McGee reactor was modeled in FLUENT without the scouring agent and the initial points of deposition were identified. A chlorine gas-blanket inlet was added to the current Kerr-McGee reactor immediately upstream of the initial points of deposition and inlet conditions of the chlorine gas were set to equilibrate the momentum of the oxygen stream with the chlorine stream. The results of the analysis show that although the addition of the gas increases the turbulence and mixing rate downstream in the reactor, it will not, with the given flow rate and design angle, prevent oxide accretion on the reactor wall.

A recommendation for future study is to decrease the angle of the chlorine inlet and to adjust the chlorine flow rate as needed, preferably to $26.5\cos\theta$ (m/s) where θ is the

angle between the chlorine inlet and the axial line of the reactor. Decreasing θ should serve to keep the chlorine gas closer to the reactor wall where needed and out of the bulk fluid, and serve to decrease the amount of chlorine required, thereby preserving the particle size distribution.

To prevent deposition, Kerr-McGee requires no more than a 10% increase in chlorine gas in the system. With the altered design, there is an 80% (by mass) increase of chlorine in the system. Reducing the angle of the chlorine gas inlet to nearly parallel with the axial direction of the reactor would reduce the required chlorine by half. Therefore, the minimum chlorine deliverable to prevent deposition on just the TiCl_4 nozzle area causes an increase of chlorine in the reactor of 40%. With the dimensions used for the chlorine gas inlet, a chlorine gas wall sheath cannot be used for the reduction of wall scale and remain under the limit of chlorine gas in the system.

REFERENCES

- Aggus, B., "Analysis of Reactors for the Production of Titanium Dioxide through Computational Fluid Dynamics," M.S. Thesis, Department of Chemical Engineering, Oklahoma State University, Stillwater, Oklahoma (2000).
- Akhtar, M.K., Xiong, Y. and Pratsinis, S.E., "Vapor Synthesis of Titania Powder by Titanium Tetrachloride Oxidation," *AIChE Journal* 37 (10), 1561-1570 (1991).
- Aspen Plus® V.10, Aspen Technology, Inc., Cambridge, Massachusetts (1999).
- Bedetti, G., Montecatini Edison S.p.A., "Apparatus for the Combustion of Titanium Tetrachloride with Oxygen for the Production of Titanium Dioxide Pigment," U.S. Patent 3,676,060 (1972).
- Bedetti, G., Montecatini Edison S.p.A., "Process for the Combustion of Titanium Tetrachloride with Oxygen for the Production of Titanium Dioxide," U.S. Patent 3,552,920 (1971).
- Bird, R.B., Stewart, W.E., and Lightfoot, E.N., Transport Phenomena, John Wiley and Sons, New York (1960).
- Braun, J.H., "Titanium Dioxide-A Review," *Journal of Coating Technology* 69 (868), 59-72 (1997).
- Carpenter, C. L. R., Cabot Corporation, "Apparatus and Process for the Production of Titanium Dioxide," U.S. Patent 3,203,762 (1965).
- Chang, Y.C., Ranade, M.B., and Gentry, J.W., "Thermophoretic Deposition of Aerosol Particles on Transport Tubes," *Journal of Aerosol Science* 21, 581-584 (1990).
- FLUENT 5, Fluent Incorporated, Lebanon, New Hampshire (1998).
- FLUENT 5, FLUENT User's Guide, 1-4, Fluent Incorporated, Lebanon, New Hampshire (1998).
- Goodgame, T. H., et al., Cabot Corporation, "Production of Pyrogenic Pigments," U.S. Patent 3,311,452 (1967).
- Hartmann, A., Kronos, Inc., "Process for the Production of Titanium Dioxide," U.S. Patent 5,196,181 (1993).
- Jang, H.D. and Jeong, J., "The Effects of Temperature on Particle Size in the Gas Phase Production of TiO₂," *Aerosol Science Technology* 23, 553-560 (1995).

Jang, H.D., Kim, S.K., and Han, Y.S., "Modeling on Formation of Ultrafine Titanium Dioxide Particles by Gas Phase Reaction," *Journal of Aerosol Science* 26, S562-S564 (1995).

Jain, S., Kodas, T.T., Wu, M.K. and Preston, P., "Role of Surface Reaction in Aerosol Synthesis of Titanium Dioxide," *Journal of Aerosol Science* 28 (1), 133-146 (1997).

Kerr-McGee Corporation, <http://www.Kerr-McGee.com/tio2.html> (2000).

Kobata, A., Kusakabe, K. and Morooka, S., "Growth and Transformation of TiO_2 Crystallites in Aerosol Reactor," *AIChE Journal* 37 (3), 347-359 (1991).

Kodas, T.T., and Friedlander, S. K., "Design of Tubular Flow Reactors for Monodisperse Aerosol Production," *AIChE Journal* 34 (4), 551-557 (1988).

Kruse, W. E., E. I. du Pont de Nemours and Company, "Pigmentary TiO_2 Manufacture," U.S. Patent 3,284,159 (1966).

Morooka, S., Yasutake, T., Kobata, A., Ikemizu, K., and Kato, Y., "A Mechanism for the Production of Ultrafine Particles of TiO_2 by a Gas-Phase Reaction," *International Chemical Engineering* 29 (1), 119-126 (1989).

Nutting, R. D., E. I. du Pont de Nemours and Company, "Metal Oxide Production," U.S. Patent 2,670,272 (1954).

Olson, C. M., Tully, J. N., E. I. du Pont de Nemours and Company, "Metal Oxide Production," U.S. Patent 2,915,367 (1959).

Pieri, G., Ducato, A., Held, L. J., Bedetti, J., Montecatini Edison S.p.A. and The New Jersey Zinc Co., "Process for Producing Pigment Quality Titanium Dioxide," U.S. Patent 3,725,526 (1973).

Powell R., "Titanium Dioxide and Titanium Tetrachloride," *Chemical Process Review* 18 (1968).

Pratsinis, S.E., "Simultaneous Nucleation, Condensation, and Coagulation in Aerosol Reactors," *Journal of Colloid and Interface Science* 124 (2), 416-427 (1988).

Pratsinis, S.E., Bai, H. and Biswas, P., "Kinetics of Titanium(IV) Chloride Oxidation," *Journal of the American Ceramic Society* 73 (7), 2158-2162 (1990).

Pratsinis, S.E., Kodas, T.T., DudoKovic, M.P., and Friedlaner, S.K., "Aerosol Reactor Design: Effect of Reactor Geometry on Powder Production and Vapor Deposition," *Powder Technology* 47, 17-23 (1986).

Pratsinis, S.E. and Spicer, P.T., "Competition Between Gas Phase and Surface Oxidation of TiCl_4 during Synthesis of TiO_2 Particles," *Chemical Engineering Science* 53 (10), 1861-1868 (1997).

Pratsinis, S.E., Zhu, W. and Vemury, S., "The Role of Gas Mixing in Flame Synthesis of Titania Powders," *Powder Technology* 86, 87-93 (1996).

Sadakata, M., Xu, Y.B. and Harano, A., "A Systematic Approach for the Design of Aerosol Reactors," *Powder Technology* 88, 261-266 (1996).

Seto, T., Shimada, M., and Okuyama, K., "Evaluation of Sintering of Nanometer-Sized Titania Using Aerosol Method," *Aerosol Science and Technology* 23, 183-200 (1995).

Shay, C.D., "Design and Optimization of a High Temperature Reactor for the Production of Group II-VI Compounds Via Computer Models and Statistical Experimentation," M.S. Thesis, Department of Chemical Engineering, Oklahoma State University, Stillwater, Oklahoma (1998).

Wendell, C. B., Carpenter, C. L. R., Greene, M. J., Cabot Corporation, "Vapor Phase Process for Producing Metal Oxides," U.S. Patent 3,351, 427 (1967).

Wilson, W. L., PPG Industries, Inc., "Method and Apparatus for Distribution of Gases in an Annulus," U.S. Patent 3,586, 055 (1971).

Xiong, Y., Akhtar, M.K. and Pratsinis, S.E., "Formation of Agglomerate Particles by Coagulation and Sintering—Part II. The Evolution of the Morphology of Aerosol-Made Titania, Silica and Silica-Doped Titania Powders," *Journal of Aerosol Science* 24 (3), 301-313 (1993).

APPENDIX A

Additional Cabot Results

CASE I

Figure 54 presents the two-dimensional density profile of the Case I Cabot reactor. The density ranges from 0.7 to 16.3 kg/m³ and is the lowest in the oxygen inlet and is highest in the titanium tetrachloride inlet.

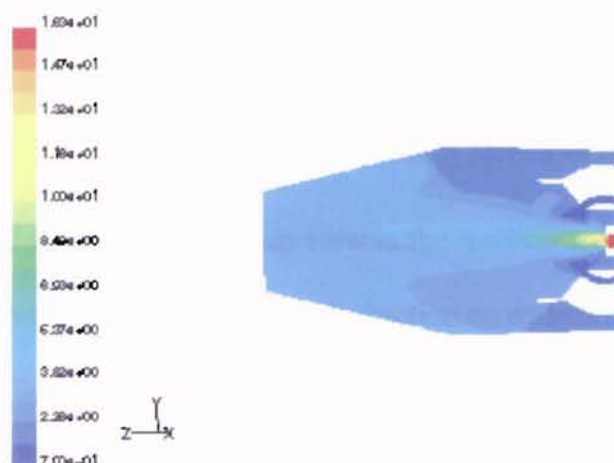


Figure 54 (Cabot Case I) Density Profile

Figure 55 presents the turbulent rate of reaction (kmol/s) and qualitatively where the reaction takes place in the reactor.

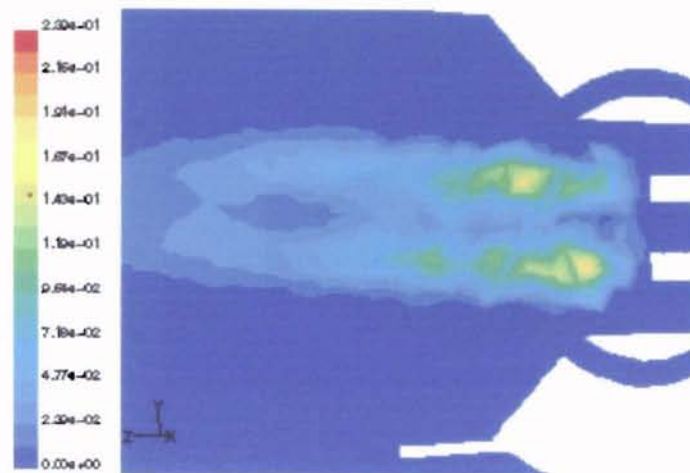


Figure 55 (Cabot Case I) Reaction Profile

Figure 56 presents a close-up view in the reaction area of the mole fraction of titania and shows a non-zero titania mole fraction on several of the reactor surfaces.

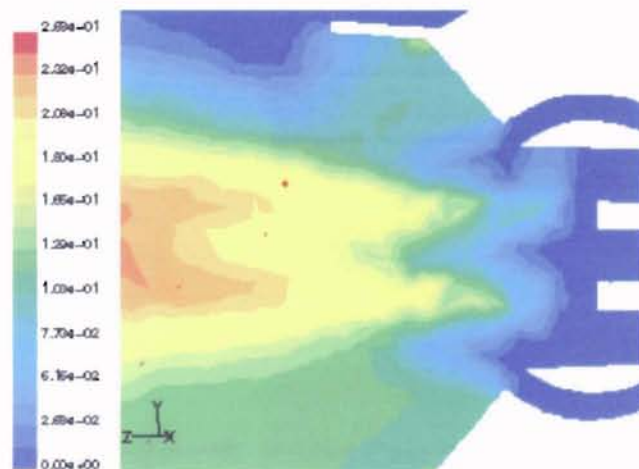


Figure 56 (Cabot Case I) Close-up Mole Fraction TiO_2

Figure 57 and Figure 58 present the pressure profile in Pascal (gage) and the velocity profile in m/s of the Case I Cabot reactor.

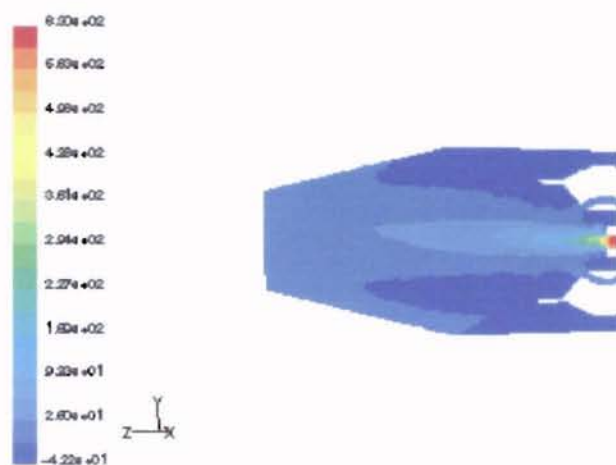


Figure 57 (Cabot Case I) Pressure Profile

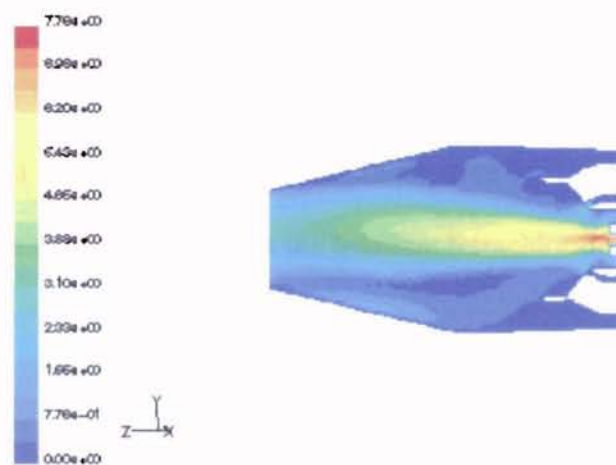


Figure 58 (Cabot Case I) Velocity Profile

Figure 59 presents a close-up view of the velocity vectors in the reaction region of the Case I Cabot reactor. Velocity vectors are useful in identifying regions of backflow and swirling.

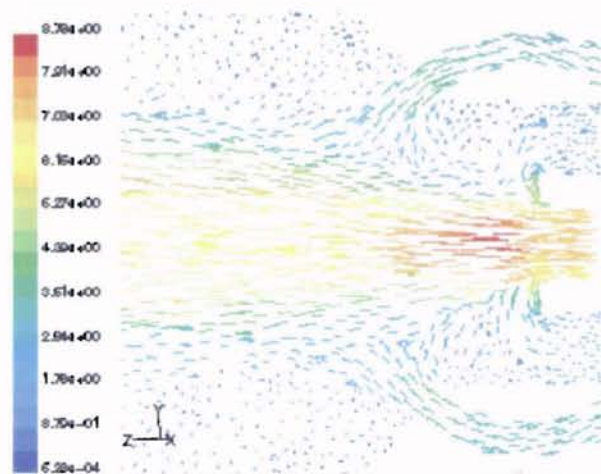


Figure 59 (Cabot Case I) Close-up Velocity Vector Profile

CASE II

Figure 60 presents the two-dimensional density profile of the Case II Cabot reactor. Like all other cases, the density ranges from 0.7 to 16.3 kg/m^3 and is the lowest in the oxygen inlet and is highest in the titanium tetrachloride inlet.

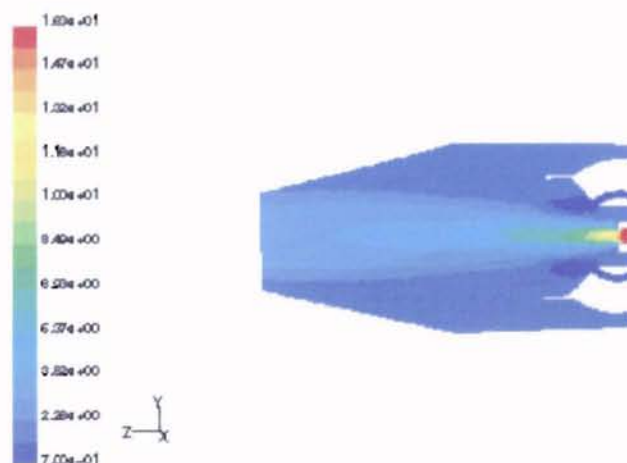


Figure 60 (Cabot Case II) Density Profile

Figure 61 presents the pressure profile of the Case II Cabot reactor. Comparing Case II to Case I, it can be seen that the inner chlorine stream does not have to overcome the higher pressure of the oxygen inlet seen in Case I and the chlorine gas is able to drive the oxygen downstream.

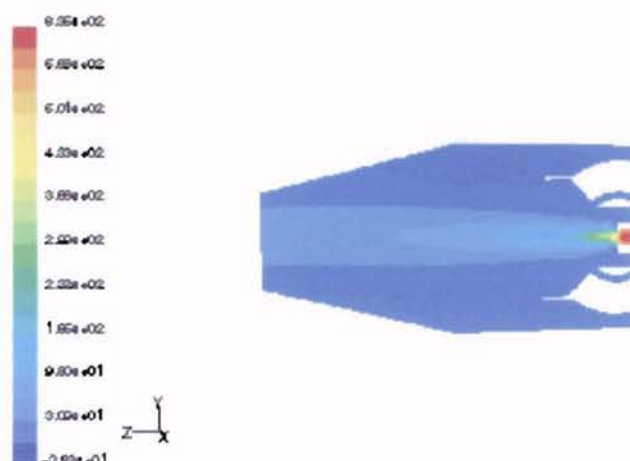


Figure 61 (Cabot Case II) Pressure Profile

Figure 62 presents the reaction rate profile for Case II and in three dimensions would appear as an annulus down the center of the reactor.

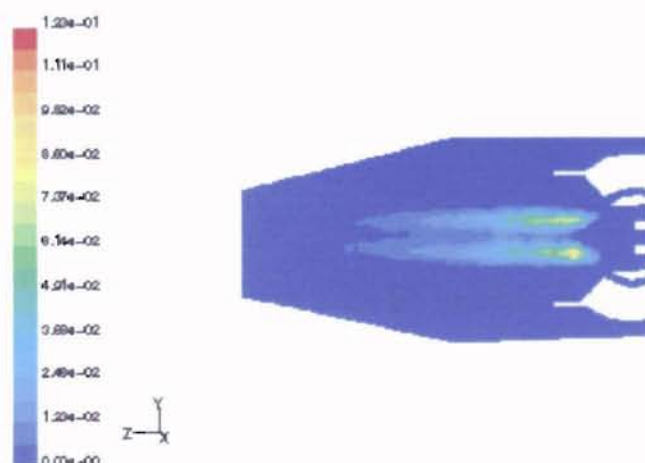


Figure 62 (Cabot Case II) Reaction Profile

Figure 63 presents the velocity profile for Case II Cabot reactor and ranges from 0 (no slip at the wall boundary condition) to 7.61 m/s.

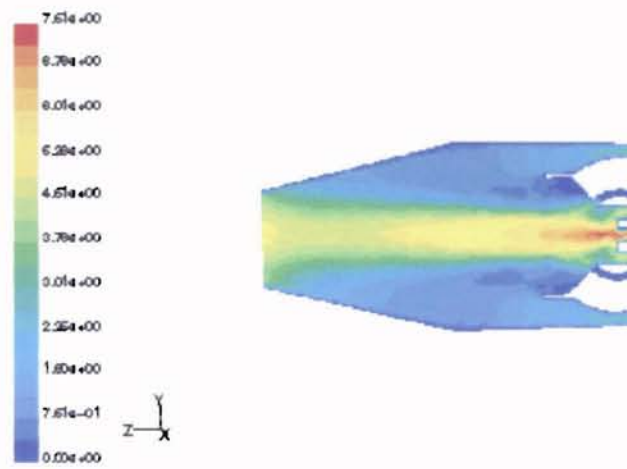


Figure 63 (Cabot Case II) Velocity Profile

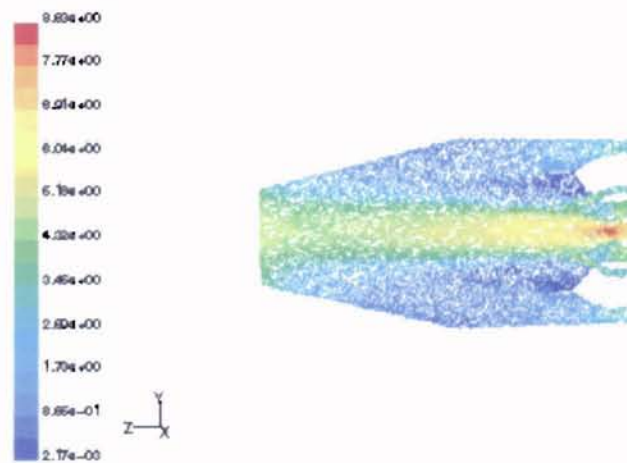


Figure 64 (Cabot Case II) Velocity Vector Profile

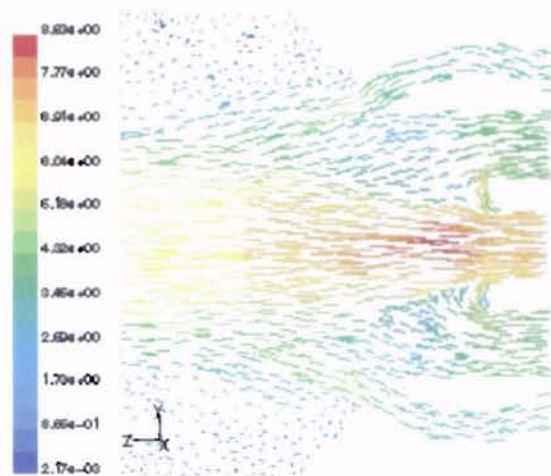


Figure 65 (Cabot Case II) Close-up Velocity Vector Profile

CASE III

Figure 66 presents the two-dimensional density profile of the Case III Cabot reactor. It can be confirmed in this figure that the locations of the chloride and oxygen inlets have been switched.

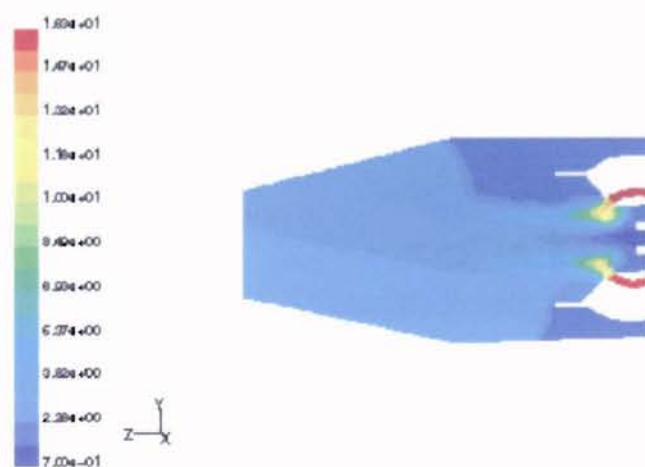


Figure 66 (Cabot Case III) Density Profile

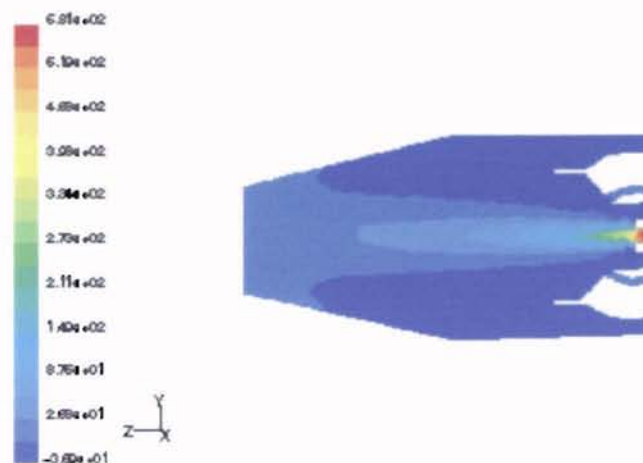


Figure 67 (Cabot Case III) Pressure Profile

Figure 68 presents the turbulent reaction profile for Case III and is similar to that of Case I. It can be seen from all Cabot reaction profiles that reaction does not readily occur on the wall surfaces.

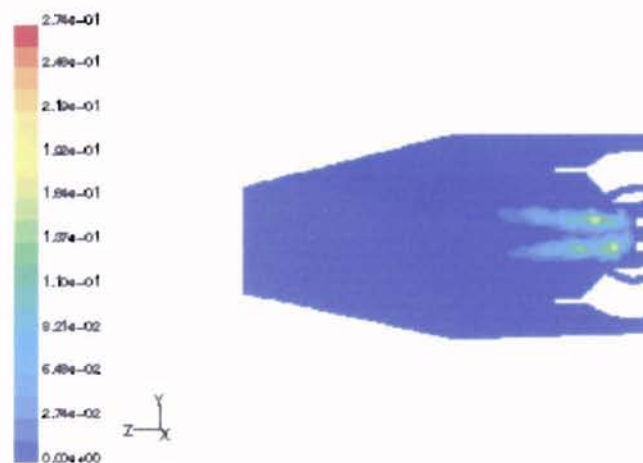


Figure 68 (Cabot Case III) Reaction Profile

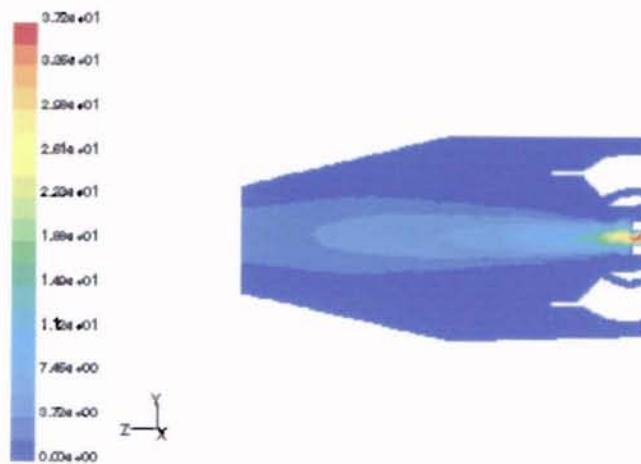


Figure 69 (Cabot Case III) Velocity Profile

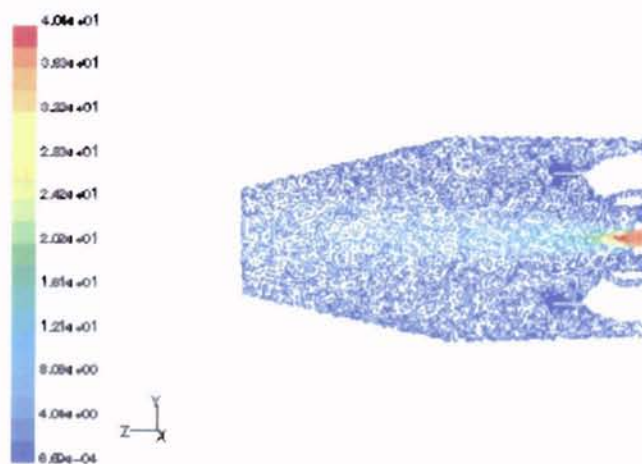


Figure 70 (Cabot Case III) Velocity Vector Profile

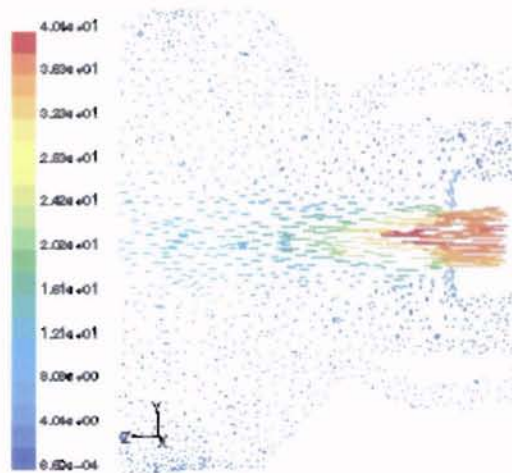


Figure 71 (Cabot Case III) Close-up Velocity Vector Profile

CASE IV

Figure 72 presents the density profile of the Cabot Case IV reactor. The higher flow rate of chlorine sweeps the chloride further downstream and away from the inlets.

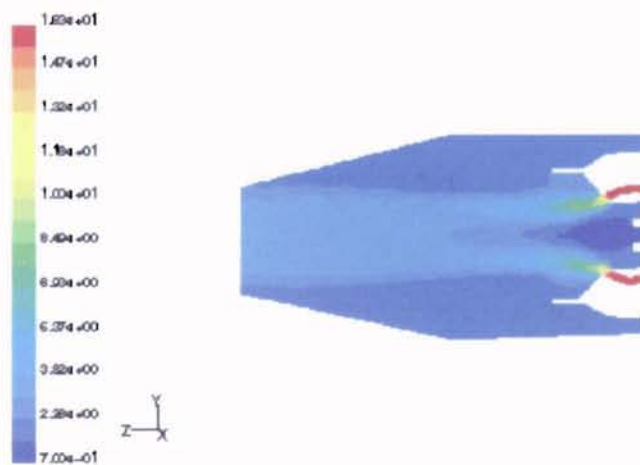


Figure 72 (Cabot Case IV) Density Profile

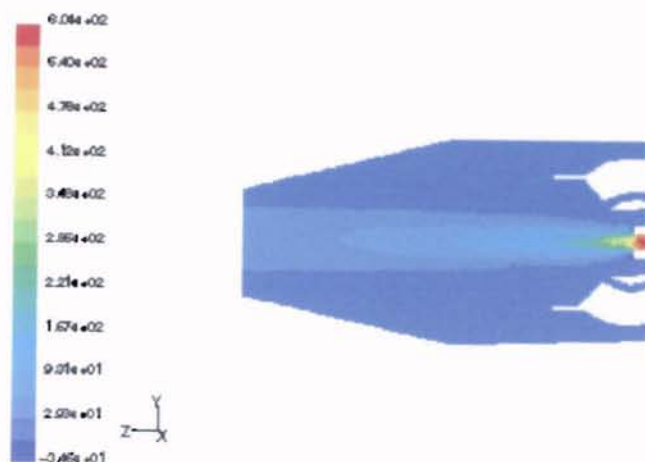


Figure 73 (Cabot Case IV) Pressure Profile

Figure 74 presents the reaction rate profile for the Cabot Case IV reactor. Compared to Case II, Figure 62, this reaction profile is in a more defined annular shape due to the change of reactant inlet positions.

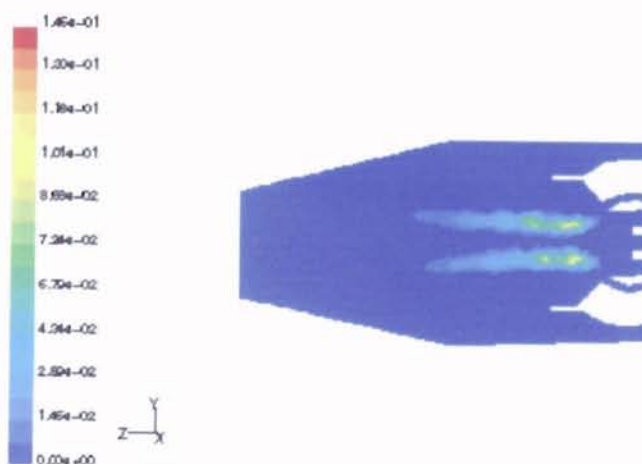


Figure 74 (Cabot Case IV) Reaction Profile

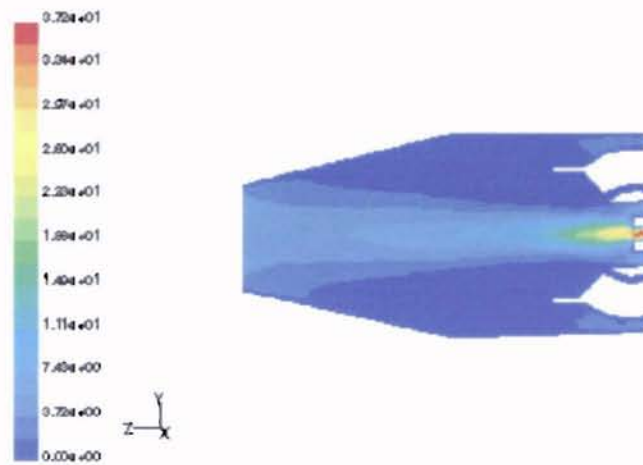


Figure 75 (Cabot Case IV) Velocity Profile

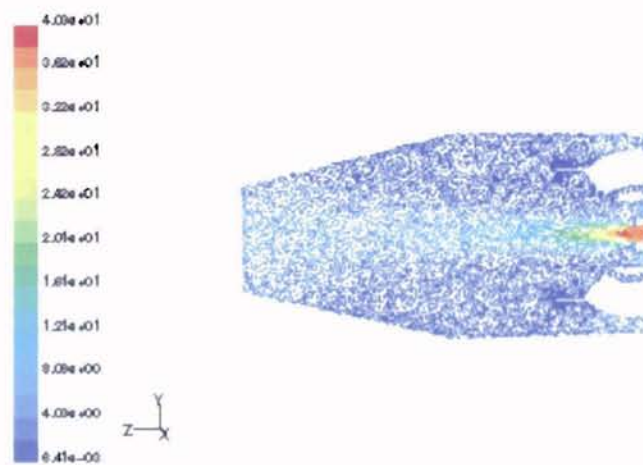


Figure 76 (Cabot Case IV) Velocity Vector Profile

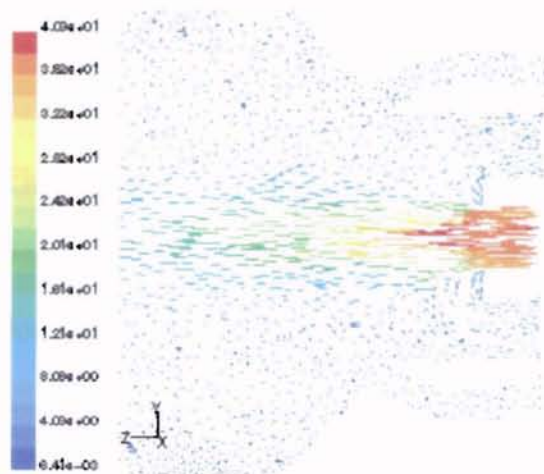


Figure 77 (Cabot Case IV) Close-up Velocity Vector Profile

APPENDIX B

Additional PPG Results

Low Chlorine Flow (Case I)

Figure 78 presents the density profile of the Case I PPG reactor profile. The high density red region is clearly pure titanium tetrachloride and the dark blue region is low density oxygen.

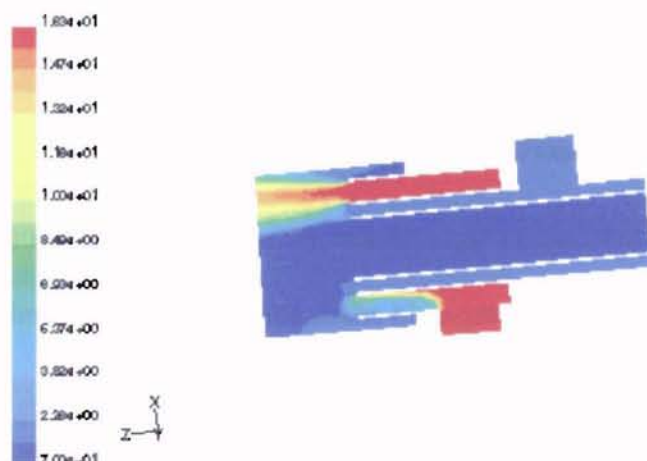


Figure 78 (PPG Reactor Case I) Density Profile

Figure 79 presents the pressure profile for the PPG Case I reactor. The titanium tetrachloride is being fed at a higher pressure than the oxygen and the pressure differential across the chloride annulus can be seen in the figure.

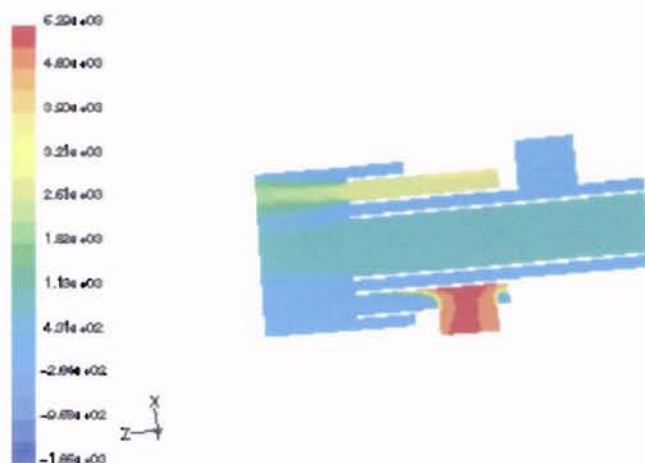


Figure 79 (PPG Reactor Case I) Pressure Profile

Figure 80 presents the turbulent reaction rate of the PPG reactor for Case I. Qualitatively, the reaction takes place in the blue-green region and near the annulus wall separating the oxygen inlet and the chlorine inlet.

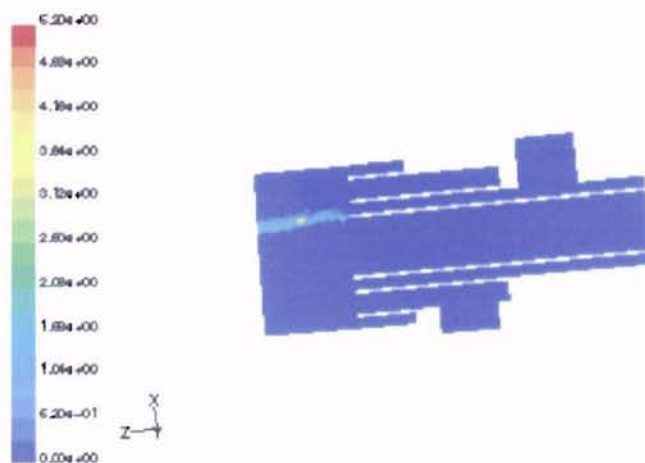


Figure 80 (PPG Reactor Case I) Reaction Profile

Figure 81 and Figure 82 present the velocity magnitude and velocity vector profiles, respectively. The oxygen is delivered at the highest velocity at 62.3 m/s.

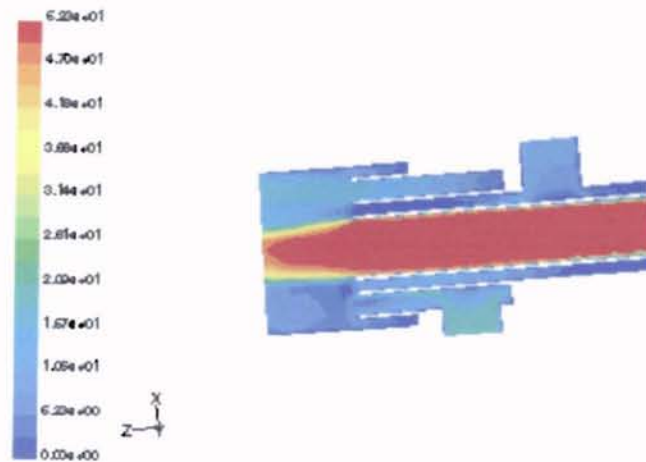


Figure 81 (PPG Reactor Case I) Velocity Profile

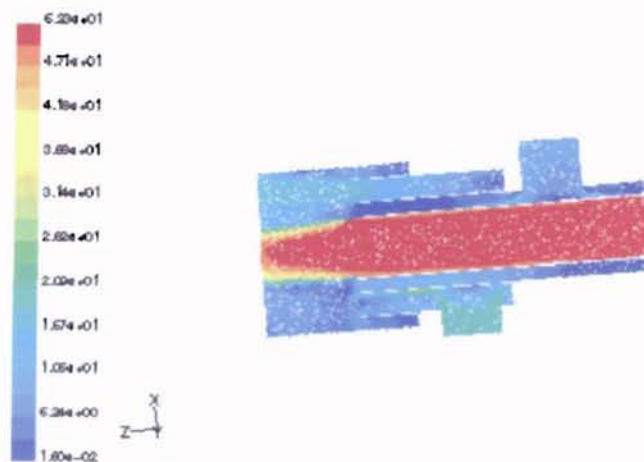


Figure 82 (PPG Reactor Case I) Velocity Vector Profile

High Chlorine Flow (Case II)

Figure 83 presents the density profile of the Case II PPG reactor profile.

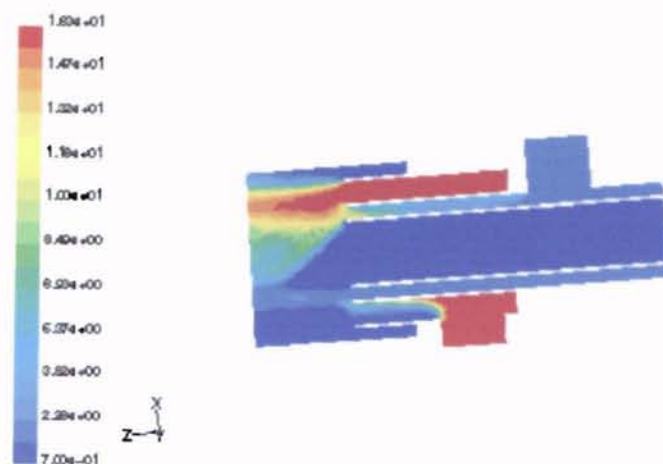


Figure 83 (PPG Reactor Case II) Density Profile

In Case II, the delivery pressure of the chlorine gas exceeds that of the chloride gas as seen in Figure 84.

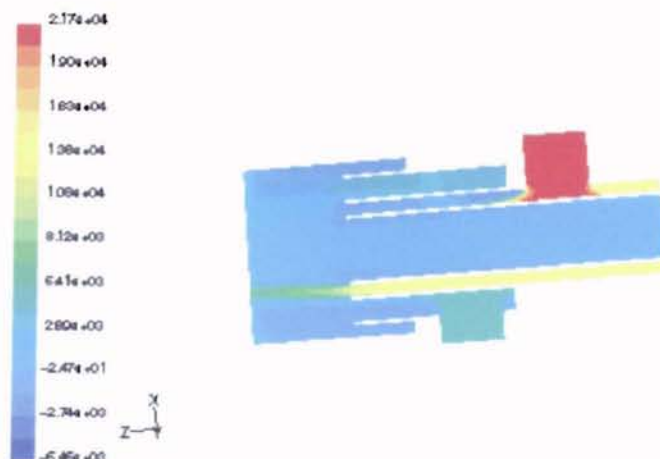


Figure 84 (PPG Reactor Case II) Pressure Profile

Figure 85, compared with Figure 80, shows that less reaction is taking place in Case II than in Case I. Figure 85 also shows that reaction is taking place in the chlorine inlet and most quickly on the reactor wall.

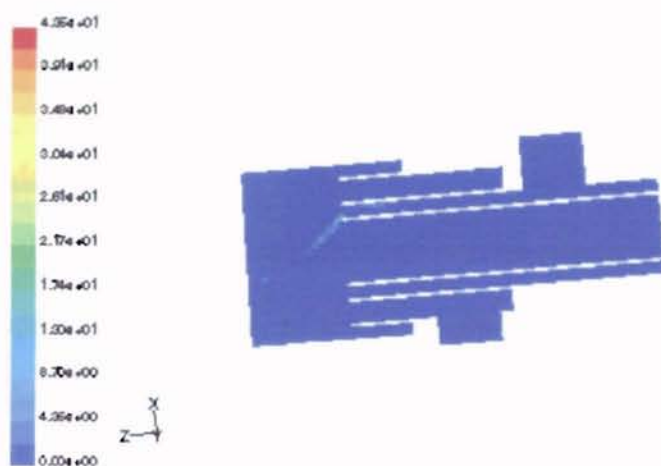


Figure 85 (PPG Reactor Case II) Reaction Profile

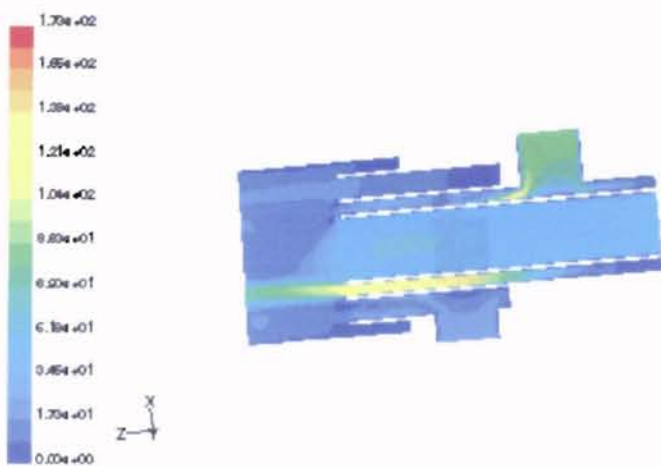


Figure 86 (PPG Reactor Case II) Velocity Profile

APPENDIX C

Additional Kerr-McGee Results

Original Kerr-McGee Reactor

The density profile for the original Kerr-McGee reactor is presented in Figure 87 and can be compared to the density profile of the altered Kerr-McGee reactor, Figure 91. The orange in the upper side of the titanium tetrachloride spool can only be explained by convergence error.

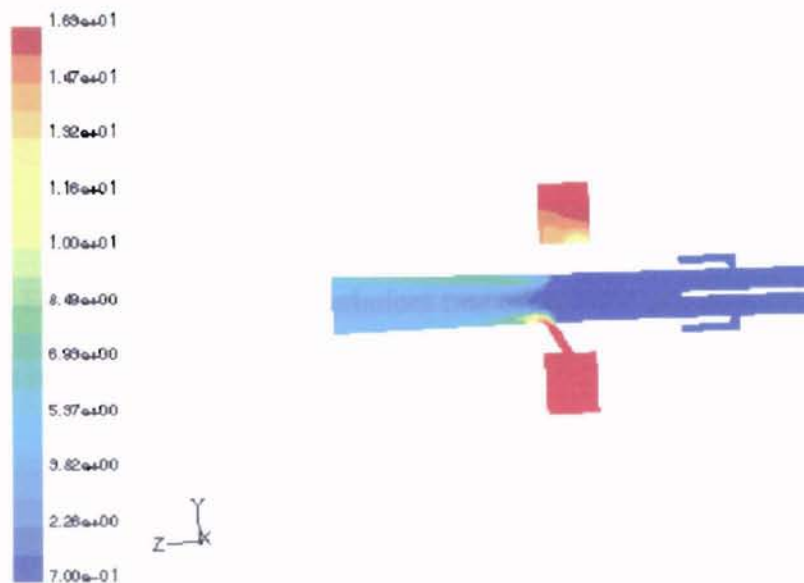


Figure 87 (Kerr-McGee Reactor) Density Profile

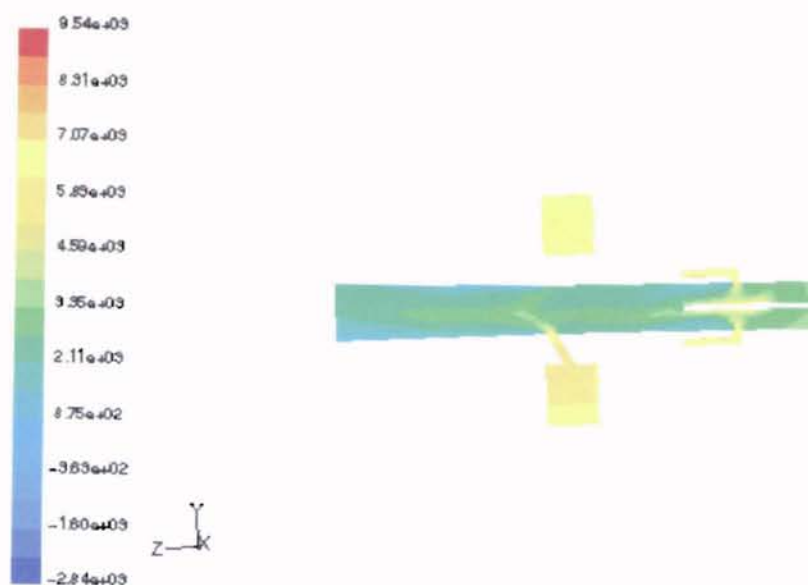


Figure 88 (Kerr-McGee Reactor) Pressure Profile

Figure 89 presents the turbulent rate of reaction profile for the original Kerr-McGee reactor.

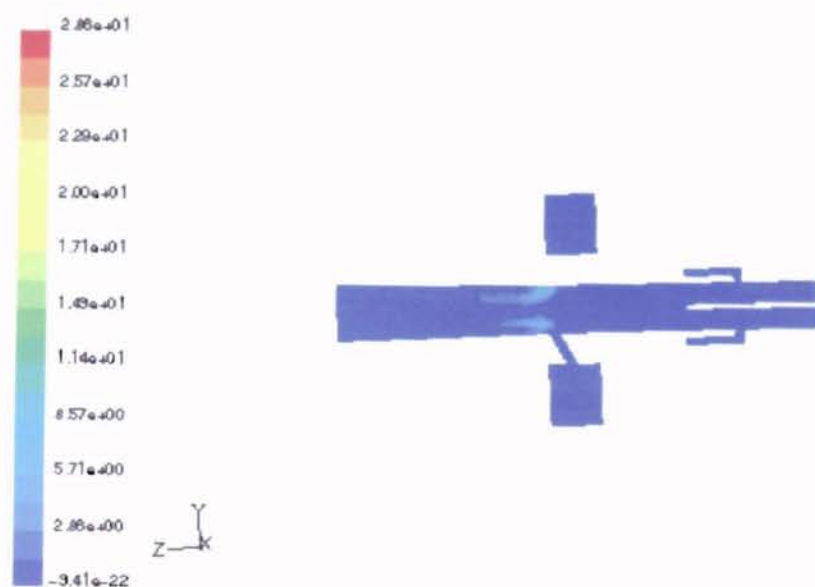


Figure 89 (Kerr-McGee Reactor) Reaction Profile

The velocity profile (m/s) for the original Kerr-McGee reactor is presented in Figure 90. Dark blue walls call attention to the no-slip boundary condition.

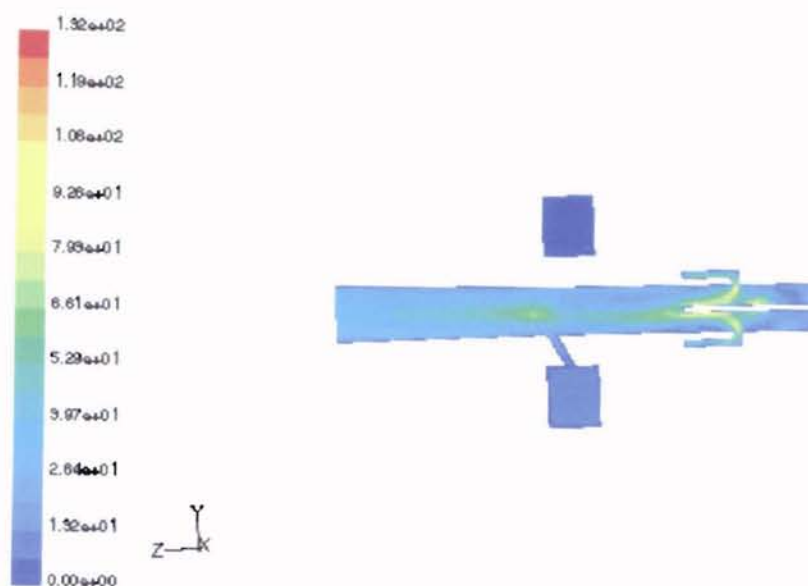


Figure 90 (Kerr-McGee Reactor) Velocity Profile

Altered Kerr-McGee Reactor

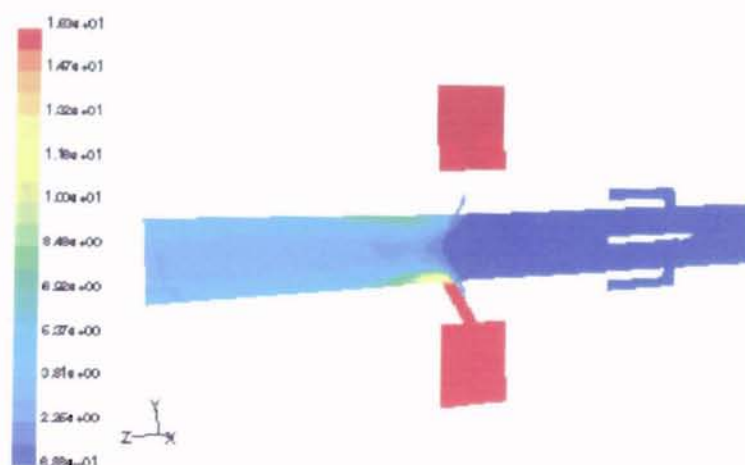


Figure 91 (Altered Kerr-McGee Reactor) Density Profile

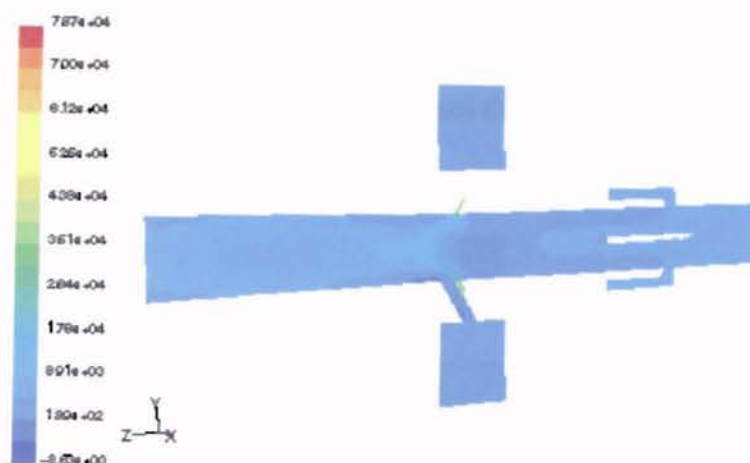


Figure 92 (Altered Kerr-McGee Reactor) Pressure Profile

Figure 93 presents the turbulent rate of reaction for the altered Kerr-McGee reactor. Compared to Figure 89, the reaction is actually occurring further away from the reactor walls.

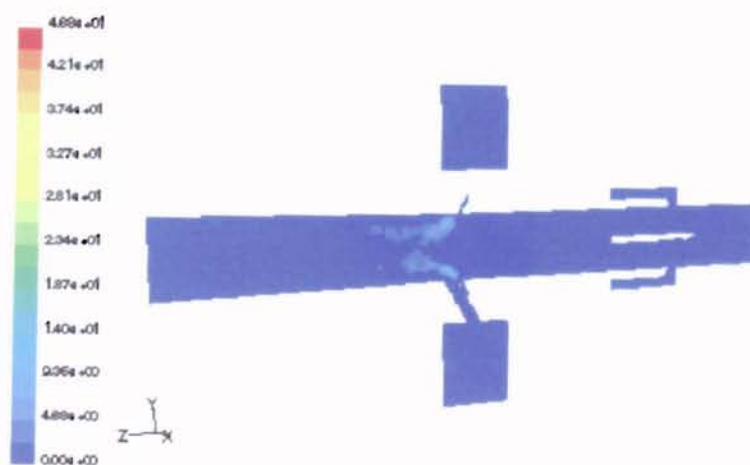


Figure 93 (Altered Kerr-McGee Reactor) Reaction Profile

Figure 94 presents the velocity magnitude profile (m/s) of the altered Kerr-McGee reactor. The addition of the chlorine gas increases the overall velocity of the system.

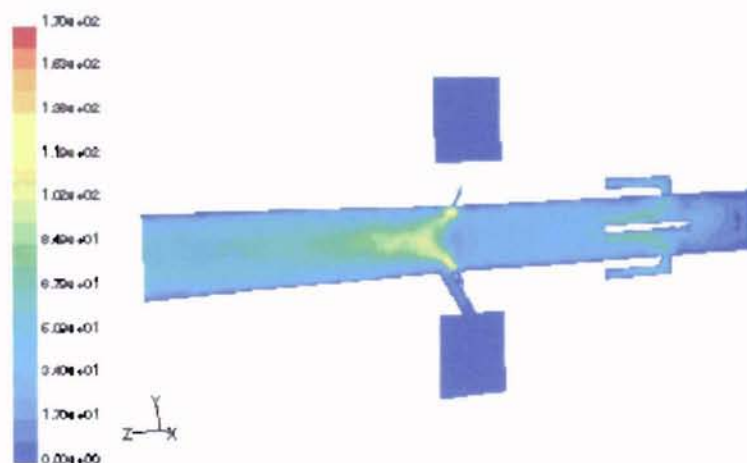


Figure 94 (Altered Kerr-McGee Reactor) Velocity Profile

APPENDIX D

Sensitivity of Diffusivity Constant

The following figures present the mole fractions of titania for two case studies where the diffusivity was fluctuated by +50% (Figure 95) and -50% (Figure 96). The analyses were performed on the altered Kerr-McGee reactor. There is very little difference in the following figures.

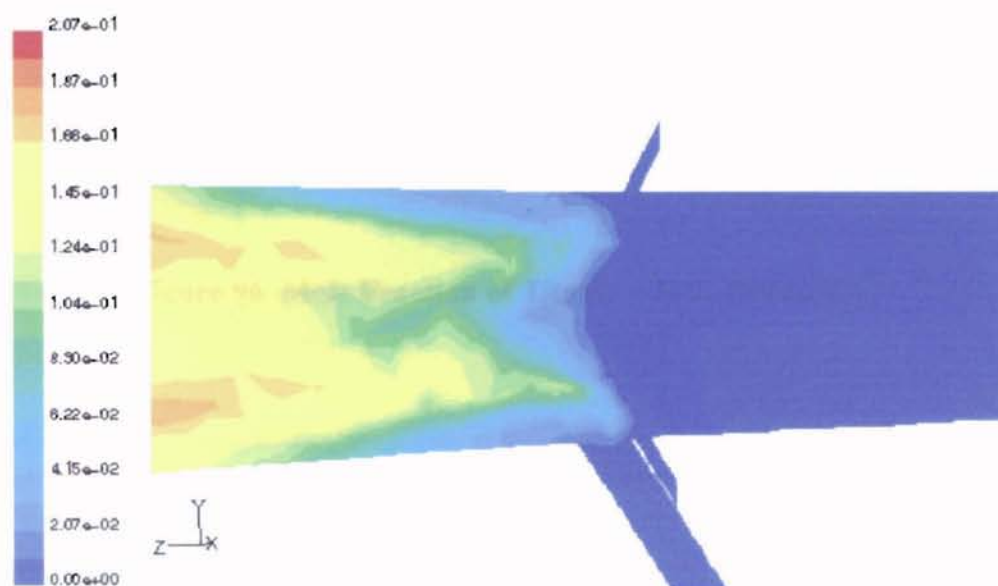


Figure 95 Mole Fraction of Titania (+50% Diffusivity)

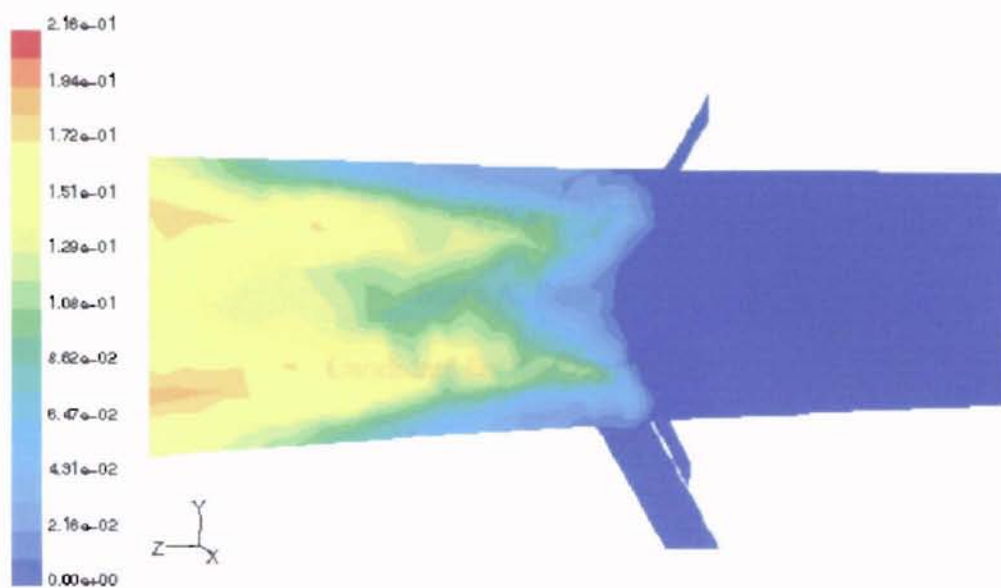


Figure 96 Mole Fraction of Titania (-50% Diffusivity)

VITA 2

Mary A. Ross

Candidate for the Degree of

Master of Science

Thesis: ANALYSIS OF CHLORIDE PROCESS REACTORS FOR THE
REDUCTION OF OXIDE SCALE THROUGH COMPUTATIONAL FLUID
DYNAMICS

Major Field: Chemical Engineering

Biographical:

Education: Received Bachelor of Science degree in Chemical Engineering from Oklahoma State University in Stillwater, Oklahoma in May 1998. Completed the Requirements for the Masters degree at Oklahoma State University in May, 2001.

Experience: Employed as a teaching assistant at Oklahoma State University School of Chemical Engineering from August 2000 to May 2001 and from January 1999 to May 1999. Employed as a research assistant at Oklahoma State University School of Chemical Engineering from May 1999 to August 2000. Employed as an intern at Conoco Inc., summer 1997.